Division of Pharmaceutical Technology
Faculty of Pharmacy
University of Helsinki
Finland

The roughness and imaging characterisation of different pharmaceutical surfaces

by

Paulus Seitavuopio

Academic dissertation

To be presented, with the permission of the Faculty of Pharmacy of the University of Helsinki, for public criticism in Auditorium 1041 at Biocenter 2 (Viikinkaari 5E) on June 8th, 2006, at 12 noon.

Helsinki 2006

Supervisors: Professor Jouko Yliruusi
Division of Pharmaceutical Technology
Faculty of Pharmacy
University of Helsinki
Finland

Docent Jukka Rantanen
Drug Discovery and Development Technology Center
Division of Pharmaceutical Technology
Faculty of Pharmacy
University of Helsinki
Finland

Reviewers: Docent Jukka-Pekka Mannermaa
Verman Oy
Järvenpää
Finland

Docent Leena Peltonen
Division of Pharmaceutical Technology
Faculty of Pharmacy
University of Helsinki
Finland

Opponent: Professor Peter Kleinbudde
Institute of Pharmaceutics and Biopharmaceutics
Heinrich-Heine-University Duesseldorf
Germany

ISBN 952-10-3117-4 (print)
ISBN 952-10-3118-2 (pdf, http://ethesis.helsinki.fi/)
ISSN 1795-7079

Helsinki University Printing House
Helsinki 2006
Finland

To Hanna & Anna

Abstract

Seitavuopio, P.J, 2006. The roughness and imaging characterisation of different pharmaceutical surfaces

Dissertationes biocientiarum molecularium Universitatis Helsingiensis in Viikki, 10/2006, pp.91, ISBN 952-10-3117-4 (print) ISBN 952-10-3118-2 (pdf) ISSN 1795-7079.

The surface properties of solid state pharmaceutics are of critical importance. Processing modifies the surfaces and effects surface roughness, which influences the performance of the final dosage form in many different levels. Surface roughness has an effect on, e.g., the properties of powders, tablet compression and tablet coating. The overall goal of this research was to understand the surface structures of pharmaceutical surfaces. In this context the specific purpose was to compare four different analysing techniques (optical microscopy, scanning electron microscopy, laser profilometry and atomic force microscopy) in various pharmaceutical applications where the surfaces have quite different roughness scale. This was done by comparing the image and roughness analysing techniques using powder compacts, coated tablets and crystal surfaces as model surfaces.

It was found that optical microscopy was still a very efficient technique, as it yielded information that SEM and AFM imaging are not able to provide. Roughness measurements complemented the image data and gave quantitative information about height differences. AFM roughness data represents the roughness of only a small part of the surface and therefore needs other methods like laser profilometer are needed to provide a larger scale description of the surface. The new developed roughness analysing method visualised surface roughness by giving detailed roughness maps, which showed local variations in surface roughness values. The method was able to provide a picture of the surface heterogeneity and the scale of the roughness. In the coating study, the laser profilometer results showed that the increase in surface roughness was largest during the first 30 minutes of coating when the surface was not yet fully covered with coating. The SEM images and the dispersive X-ray analysis results showed that the surface was fully covered with coating within 15 to 30 minutes. The combination of the different measurement techniques made it possible to follow the change of surface roughness and development of polymer coating. The optical imaging techniques gave a good overview of processes affecting the whole crystal surface, but they lacked the resolution to see small nanometer scale processes. AFM was used to visualize the nanoscale effects of cleaving and reveal the full surface heterogeneity, which underlies the optical imaging. Ethanol washing changed small (nanoscale) structure to some extent, but the effect of ethanol washing on the larger scale was small. Water washing caused total reformation of the surface structure at all levels.

Table of contents

List of original publications

Thesis based on the following original articles, which are referred to in the text by the Roman numerals as I-IV.

I Seitavuopio, P., Rantanen, J., Yliruusi, J.
Tablet surface characterization by various imaging techniques. International Journal of Pharmaceutics 2003, 254(2), 281-286.

II Seitavuopio, P., Rantanen, J., Yliruusi, J.
Use of roughness maps in visualisation of surfaces. European Journal of Pharmaceutics and Biopharmaceutics 2005, 59(2), 351-358.

III Seitavuopio, P., Heinämäki, J., Rantanen, J., Yliruusi, J.
Monitoring tablet surface roughness during the film coating process. AAPS PharmSciTech 2006, 7(2), article 31.

IV Seitavuopio, P., Aaltonen, J., Rantanen, J., Yliruusi, J.
Solvent induced morphological changes during washing on model crystal surfaces (submitted).

Acknowledgements

This study was carried out at the Pharmaceutical Technology Division, Department of Pharmacy, University of Helsinki during the years 1999-2006.

I would like to express my deep and sincere gratitude to my supervisor, Professor Jouko Yliruusi, for his guidance and encouragement during this study. I would like to thank Prof. Yliruusi for those many inspiring discussions about science and life in general. Without his warm support, patience and inspiration, this work would not have been possible.

I am sincerely grateful to Docent Jukka Rantanen for his support, understanding and never-ending optimism which helped in the difficult days of this project.

I extend my sincere thanks to Docent Jukka-Pekka Mannermaa and Docent Leena Peltonen for reviewing the manuscript and for giving valuable suggestions for its improvement.

I am most grateful to my co-authors, Docent Jyrki Heinämäki and MSc. Jaakko Aaltonen for their co-operation.

I would like express my best thanks to MSc. Flemming Jørgensen for his help and co-operation in the early days to AFM research.

I express my gratitude to all my colleagues at the Division of Pharmaceutical Technology for creating pleasant and inspiring working atmosphere. I would especially thank for your company at lunches, coffee breaks, different kinds of official and un-official trips & outings which I have had the pleasure to enjoy in good company. These events have been the life line in difficult days of research.

I gratefully acknowledge the financial support from the National Technology Agency of Finland (TEKES).

I am ever grateful to my parents Mirja and Lasse for their never-ending love and support. Finally, my warmest thanks go to my family Hanna and Anna for bringing love and laughter to my life. Without them, everything would have been much harder.

Helsinki, June 2006

Paulus Seitavuopio

1. Introduction

Surface roughness has a large influence on our daily lives since it affects many common phenomena like friction. Friction prevents us falling down when we are walking if we have enough roughness on our shoes and on the floor. Surface roughness is also important in adhesion since a root mean square (Rq) roughness of 1 μm can remove the adhesion between a rubber ball and a substrate surface (Persson et al. 2005). Nanoscale roughness is enough to remove adhesion between hard solids like metals and minerals. Therefore, surface roughness is the reason why the adhesion is not usually observed in most macroscopic phenomena.

Many surface properties such as friction (Koura 1981, Nogueira et al. 2002), surface wear (Qu et al. 2005), fluid flow in rough pipes (Hunsaker and Righmire 1947) and the functioning of vacuum seals (Kelly et al. 2001) are strictly dependent on surface roughness. In addition, surface roughness seems to be important in bioengineering for example in the joints of the bones (Tandon and Rakesh 1981) and in assimilation of the surgical implants with the body (Wennerberg 1996). Quite often small roughness is desired since small roughness reduces wear and energy loss, but when high friction is needed also the roughness should be larger.

Surface roughness also plays an import role in the living nature. For example, Lotus plant leaves has a very special surface roughness, which plays a major role in protecting the plant from contaminants (Barthlott and Neinhuis 1997; The Lotus Effect 2006). The right kind of surface roughness on the plant surface enables plants to self-clean their surfaces. This plant surface feature has been used as a model in materials science when developing new surface coating materials (Ming et al. 2005). In the human mouth, surface roughness also is important since bacterial plaque accumulates more easily on rougher surfaces than on smoother ones

(Bollen et al. 1996). On the other hand, in bone implants rougher surfaces have been shown to improve the implant's ability to attach to bone tissue (Suzuki et al. 1997).

The quality of surface finish after processing is one key quality elements in different fields of industry. In the steel industry, surface roughness is important since properties like the corrosion resistance and clean ability of the steel surfaces are dependent on surface roughness (Cochrane 2000). The cleaning and the soiling of the surfaces are affected by the surface roughness, but the best roughness range is largely dependent on the materials and application (Kloss et al. 2005; Kuisma et al. 2005). Surfaces that are flat on the subnanometer level are rare since neither nature nor industrial processes tend to cause smaller or bigger defects on the surfaces while surfaces are formed (Majumdar and Bhushan 1999). Special production methods must be used in order to produce atomic scale flat surfaces.

It is quite easy to collect numerous phenomena and applications within pharmaceutical technology where surface roughness is highly important. One factor influencing powder flow is the surface roughness of the powder particles (Holgado et al. 1995). In powder flow a major issue is the adhesion of powder particles which is dependent on the surface roughness of particles, as the matter of fact, the contact area between the particles (Beach et al. 2002). Friction caused by particle shape and the surface roughness is present during tablet compression (Eiliazadeh et al. 2003). The friction is sensed when powder particles adhere to each other and to the metal surfaces of the die and punches used. This friction influences the formation of the compact. The wetting characteristics and the contact angle of powders are phenomena where the influence of surface roughness has to be taken into a account (Muster and Prestidge 2002). Although surface roughness is important there have been quite few studies in pharmaceutical technology concerning roughness.

In this research, the main aim was to study and quantify the surface roughness of various pharmaceutical systems, where surface roughness exists in very different scales. The image information obtained by various techniques was used to support the roughness information. In this study the term “image” was used to describe the optical microscope, scanning electron microscope, laser profilometer and atomic force microscope images. The term “imaging characterisation” of surfaces was used to describe the information, which can be received by studying the different kinds of images produced by the techniques used in this study.

2. Review of the literature

Since surface roughness is important in so numerous phenomena and applications, it was challenging to select the proper points of view for the study. The literature review is organized in the following manner.

The main emphasis will be paid to those measuring techniques, which have been applied in the experimental studies (I-IV), and other significant measuring techniques will only be briefly be described. In addition, the mathematical theory of roughness will be limited to those practical models which really have been applied in the experiments described this study. Thus, for example, the mathematical theory of autocovariance function and the power spectral density function will not be discussed here though they have been quite widely used in roughness analysis. On the other hand, a fairly comprehensive description of them can be found in the textbooks such as Thomas, 1999.

2.1 2D surface imaging

The simplest way to characterise surface structure is visual inspection. The naked eye can tell quite much about larger scale features. The resolution of the human eye is limited to slightly under 100 µm.

2.1.1 Optical microscopy

The first optical compound microscope developed by Hooke in 1664 enhanced visual resolution greatly (Hooke 1664). The same three-lens set up is used in current microscopes. Since then of course the quality of microscope lenses has improved enormously. Optical microscope image is basically similar to the normal camera, where lighting and shadows play big part in the image. The lighting of the sample and the shadows that are created on the surface dictate what can be seen. In the optical microscope the field of view, magnification and depth of focus go together because when magnification is increased, field of view and depth focus became smaller. The theoretical resolution limit of a typical compound optical microscope is tied to the light wavelength, the resolution is about half the light wavelength. This means a maximum theoretical resolution of approximately 200 nm (Majumdar and Bhushan 1999). In practise the optical microscope can separate 1 µm lateral length scales. In recent years, some novel optical microscopic techniques have emerged which have resolutions in the region of 30-100 nm, but these techniques differ from common optical microscopes (Garini et al. 2005). Optical microscopy has been common visual screening technique in pharmaceutical dosage forms (Jacob 1999). This method is fast and inexpensive, and is a very flexible technique that works in different conditions and with a wide variety of samples. The problems with the optical microscope are its the limited resolution and small depth of focus. Optical microscopy produces only a two-dimensional view of the surface and therefore it cannot accurately describe surface topography or surface roughness.

2.1.2 Electron microscopy

Scanning electron microscopy (SEM) has usually been the next technique used when higher resolutions are needed. SEM is perhaps the most common technique in the characterisation of the drug delivery systems (Jacob 1999). The basic principle of SEM was invented in 1931 by Ernst Ruska who was awarded half of the Nobel Prize for Physics in 1986 for his invention. SEM is based on the scanning of the surface with an electron beam in a vacuum environment (Merrett et al. 2002). The schematics of SEM is described in Figure 1. When an electron beam hits the sample surface, it creates different kinds of electrons and electromagnetic waves that can be analysed. In SEM the electron beam is used as a "probe" and the surface is scanned line by line with the electron beam. The SEM image describing surface shapes is usually a result of secondary electrons emitted from the surface. The image is a computer-generated figure of the electron signals (matrix of data points), not image of light and shadows as the optical microscope image. This has be remembered since in some cases SEM images can look very similar to optical microscope images, but what the image is describes is dependent on the signal used. Other signals emitted from the sample surface can also be used to create SEM images and other data. Other commonly used signals in SEM analysis are backscatter electrons and x-ray emission signals (Bindell 1992). Backscatter electrons contrast is affected by the atom mass of the elements on the surface and x-ray emission signals can be used in elemental analysis (see below). Backscatter and x-ray emission signals are useful when surface homogeneity / heterogeneity is studied or when certain elements have to be identified on the surface. Typically SEM has a horizontal (spatial) resolution of ~5 nm and the vertical resolution of 10-20 nm (Bhushan 2001). Compared with the optical microscope SEM has much better resolution, but also much better contrast and depth of focus.

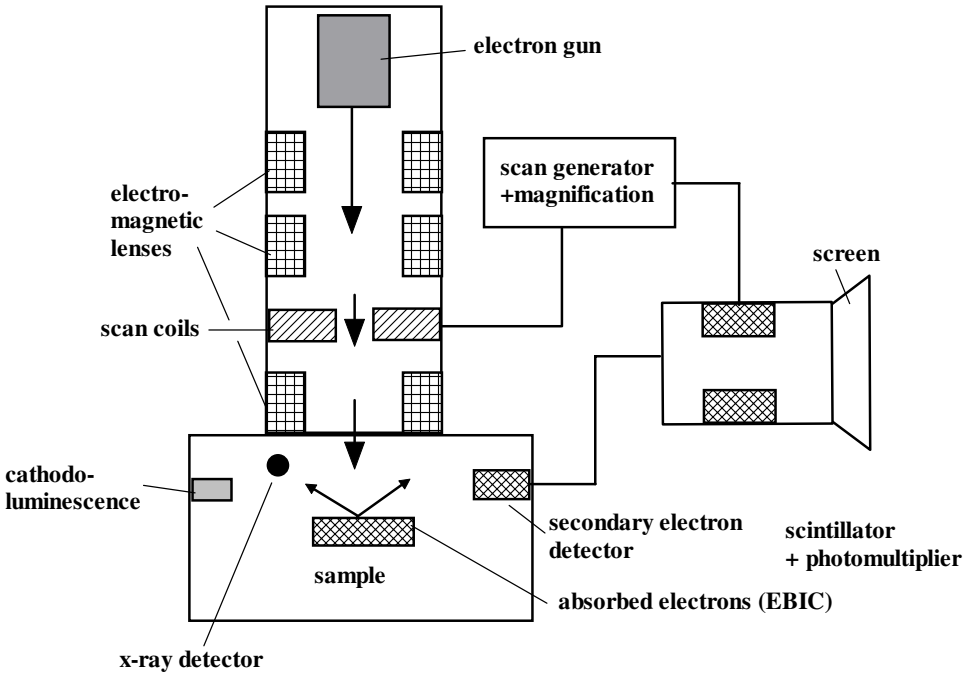

Figure 1. Schematics of SEM.

These features are especially useful when the good overall view of the sample is needed. SEM is well suited for the imaging of surfaces since it can not see through the sample like the transmission electron microscope (TEM). The sample surface orientation is more flexible in a SEM compared to the atomic force microscope, where the sample has to horizontal. In addition, sample shape usually does not cause as much problems as in atomic force microscope. The scanning electron microscope is an accurate and flexible technique, but samples have to be coated and must be vacuum compatible. The problems with sample coating and conductivity can sometimes cause artefacts in the images. Water or moisture in the sample can cause problems because ultra high vacuum is a very efficient dryer. Drying or the high vacuum itself might destroy or significantly change the sample surface. In addition, care must be taken if the materials are sensitive to heat since they can melt or burn under the electron beam that can create artefacts. The SEM does not give roughness parameters or

quantitative roughness values directly but it can be used in surface roughness analysis (Chappard et al. 2003; Chinga 2002). The extraction of the quantitative roughness information from SEM images is difficult and complex because many different aspects, affect the contrast in the images e.g. electric field enhancement at sharp edges, crystallographic enhancement (ASME 1995). For extraction of the quantitative information from SEM data there are techniques like reflection/replication, integration of backscattered signals and stereomicroscopy (Bhushan 2001).

The transmission electron microscope (TEM) is another type of electron microscope, which is more accurate than SEM. TEM looks through the samples and it cannot see the surfaces as the SEM does and therefore TEM is not very useful in surface roughness characterisation (Inoeu 2002). One advantage of SEM is the possibility to combine energy dispersive X-ray analysis to the imaging. Energy dispersive x-ray analysis (EDX) or energy dispersive x-ray spectroscopy (EDS) is a method that can be used to identify and quantify small amounts of basic elements from the sample surface (Geiss 1992; Ebnesajjad and Khaladkar 2005). With the EDX technique it is theoretically possible to identity elements which are above beryllium (Z=4) in the periodic table of elements, but the identification and quantifications are improved when atomic mass is over 10 g/mol. In EDX analysis, an electron beam excites the sample surface and then atoms on the surface emit back specific wavelengths of x-rays (Ebnesajjad and Khaladkar 2005). These wavelengths are characteristic to the unique atomic structures of elements, which enables the identification and quantification of the elements.

2.2 Measurement of the roughness and 3D imaging

The measurement of the surface roughness is very technique dependent since different roughness measurement techniques have quite different measurement scales. The roughness values from the same surfaces can be very different when measured with different techniques and different settings of the measurement equipment (Poon and Bhushan 1995; Macdonald et al. 2004) (Table 1). The resolution used in the roughness measurement affects the roughness results and generally, higher resolution means higher roughness values. The resolution of the measurement on the other hand is depend on the line or pixel density of the measurements and the size of the used probe. The surface roughness measurements techniques can be divided into two main types: profiling and parameter techniques (Vorburger and Teague 1981; ASME 1995). Profiling techniques measure the surface heights point by point with a high-resolution probe that can be some kind of stylus or optical beam. These techniques are usually quantitative and accurate. The drawback of these techniques is their usually slow measurement speeds. From the data of the profiling techniques, it is possible to create a three-dimensional image of the surface and use the instrument for 3 D imaging. Parametric surface roughness measurement is usually based on the scattering of the light (Vorburger and Teague 1981; Thomas 1999). Parameter techniques can yield an average view of the surface roughness from the measured area. These techniques cannot provide point by point information since the number of the measurements made is low, but these techniques are usually very fast in comparison with the profiling techniques.

Table 1. Comparison of roughness measurement techniques (adapted from Bhushan 2001)

Method	Quantitative information	Three-Dimensional data	Resolution (nm)		Limitations
			Horizontal	Vertical	
Stylus profilometer	Yes	Yes	15-100	0.1-1	Surface damage, slow speed in 3D mapping
Optical profilometer	Yes	Yes	500-1000	5-10	Poorly reflecting surfaces
Atomic force microscopy	Yes	Yes	0.2-1	0.02	Small scanning area
Scanning electron microscopy	Limited	Yes, 1)	5	10-50	Expensive, tedious, limited data, conductive surfaces, vacuum, small scanning area
Scanning tunneling microscopy	Yes	Yes	0.2	0.02	Requires a conducting surface, small scanning area
Optical interference	Yes	Yes	500-1000	0.1-1	Poorly reflecting surfaces
Light sectioning microscopy	Limited	Yes	500	0.1-1	Qualitative
Specular reflection	No	No	10^5-10^6	0.1-1	Semiquantitative
Diffuse reflection (scattering)	Limited	Yes	10^5-10^6	0.1-1	Smooth surfaces (<100 nm)
Speckle pattern	Limited	Yes	-	-	Smooth surfaces (<100 nm)

1) with special techniques, normal SEM images not 3D.

2.2.1 Contact profilometer

Contact or stylus profilometers are the most common types of instrument that are capable of measuring surface profiles (Vorburger 1992). Stylus profilometers have a mechanical probe or a needle, which follows the surface profile on direct contact with surface. Older contact profilometers were only capable of measuring profile lines, but now days also area scanning is possible. A modern contact profilometer is very similar to the atomic force microscope (see

below), but in larger range. The height information measured by the probe is transformed in to height information by electrical sensor resulting a 2D (profile line) or 3 D (area measurement) surface height data. The probe is usually diamond with a radius of 5-10 µm but also very sharp probes (~0.1 µm) are available for some newer equipment (ASME 1995; Poon and Bhushan 1995). The lateral resolution of the instrument depends mainly on the radius of the probe (Poon and Bhushan 1995; Zahouani et al. 1998). The sampling interval and measurement line length or measurement area size also affects the lateral resolution. The vertical (or height) resolution depends on the mechanical noise and the type of the transducer which detects the movements of the probe (Song and Vorburger 1992). The vertical resolution with a modern contact profilometer in optimum conditions can be better than 5.0 nm (Farshad et al. 2001). In practise, the measurement scale and sample surface features affect the vertical resolution. Problems with the stylus profilometer are wear of the probe and the surface deformation of the sample that can have an effect on the results (Poon and Bhushan 1995). The stylus loading can also affect the results. The sample surface shape and orientation can also have effect on the results since mechanical probe has certain physical shape and size. This means that for instance probe cannot measure deep grooves or vertical surfaces. Artefacts can occur if the surface shapes are sharper or smaller than the size of the probe. In addition, the mechanical scanning over the surface is a slow measurement technique compared to parameter techniques described below (Blunt and Rosén 2001).

2.2.2 Optical profilometer

Optical profilometers, which are also called non-contact profilometers, do not have a mechanical probe that touches the surface. Instead of a probe they use a light beam that scans the surface (Vorburger 1992). This is real advantage since the surface remains in tact after the

measurement. Optical profilometers can be divided into two main types: focus detection profilometers and interferometric profilometers. In the focus detection profilometers the beam is projected on to the surface and the focus lens keeps the beam in focus with the surface by moving the lens vertically (Depuy 1967/68; Brown 1995; Blunt and Rosén 2001) (Fig. 2).

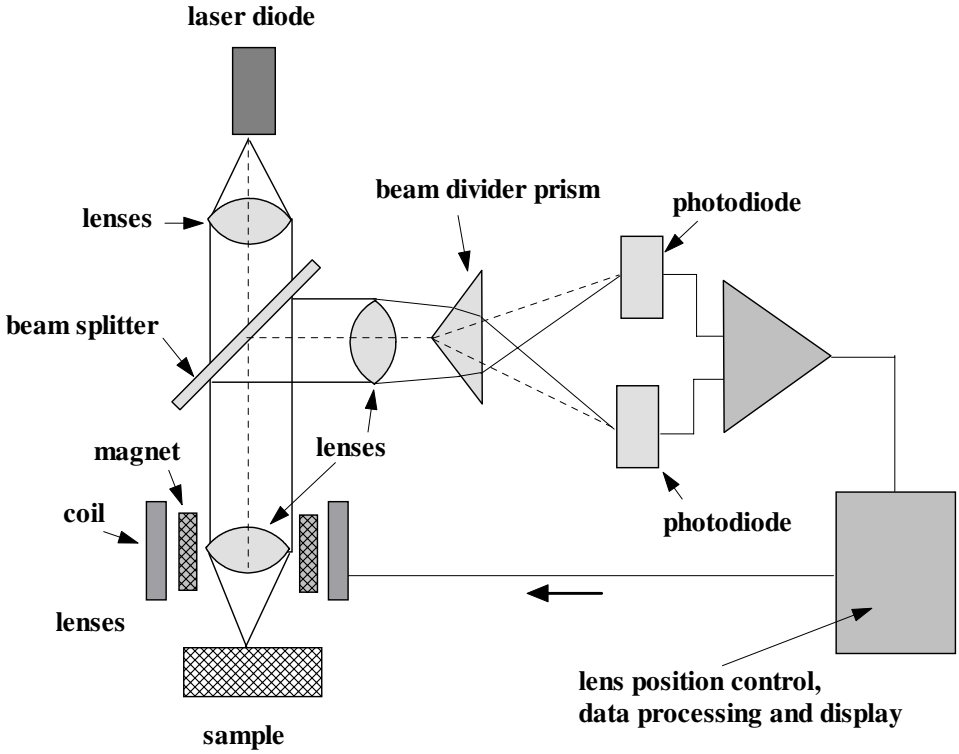

Figure 2. The schematics of optical profilometer based on focus detection.

The movement of the lens represents the height changes of the surface and the height data is generated from the lens movement signal. This type of optical profilometer is often called as a laser profilometer. In simple terms, the measurement is based distance measurement by laser beam, which reflects back to the sensor from the sample surface. The reflected signal is compared by the photodiodes to a reference beam from the laser diode. This means that surfaces that reflect light poorly or disperse the light beam way from the sensor cannot be

measured. This is a negative aspect of the optical systems because optical profilometers require at least 2% of reflection back from the surface (Brown 1995; Blunt and Rosén 2001). Besides the roughness information, the laser profilometers can also simultaneously record the strength of reflection, which is reflected back to sensor from the sample surface. The reflection signal is defined so that the 100% reflection can be received from good quality mirror surface. This reflection information is a representation of surface reflection properties materials and surface roughness. The reflection information can used for instance as a qualitative tool to separate different kinds of areas on the surface.

Steep slopes on the surfaces can cause measurement problems because in the slopes the system can lose its focus on the surface. The system tries to regain the focus from the whole z range (vertical range) and this can cause points where the surface data is false. Similarly, to the contact profilometer sample surface orientation and surface shape (e.g. sphere) can make the measurement difficult or impossible. The lateral resolution of the laser profilometer is limited to the size of the optical beam, which usually is 0.5-1 µm and the height resolution in laser profilometers is about 0.1 µm. The measurement area of the laser profilometer is from ~1 mm to several centimetres and the vertical range usually up to 1 mm. The limiting factor in lateral resolution is often measurement time limitations, because measurement of large areas with high resolution is time consuming. Often laser profilometers cannot use the maximal vertical resolution, if the measurement range is above 100 µm. Even though laser profilometers are slightly faster than traditional contact profilometers they still are slow compared to the parametric methods. Still laser profilometers can give good overall view of the surface roughness in reasonable time, but the technique has also high resolution capability.

The interferometric profilometers or simply interferometers are based on light interference phenomenon. The most common one, the two-beam interferometer, is based on the interference of two light beams where at least one of the beams is reflected back from the surface (Bhushan 2001; Blunt and Rosén 2001). It works by forming an interference pattern between a reference beam and a measuring beam. The two most common types of interferometric profilers are the phase shifting interferometer and vertical scanning interferometer (Bruning et al. 1974; Wyant et al. 1986; Caber et al. 1993). A modern commercial interferometric profiler can usually use both phase shifting and vertical scanning techniques (Harasaki et al. 2001). The phase shifting techniques is used for very smooth surfaces (<0.5 µm) since it has a better resolution and the vertical range of this technique is limited (Wyant 2002).

The vertical sensing technique is used for rougher samples due to its larger range (up to 500 µm). The vertical sensing interferometry is also called white light interferometry, because the light source in the vertical sensing is usually a white light source, which produces multiple wavelengths. Interferometers are capable of measuring the surface roughness on a nanometer scale, but they require surfaces that have reasonably good reflection properties. Optical profilometers based on white light interferometry can have a height resolution of 0.1 nm and lateral resolution of 0.5 µm (Le and Sutcliffe 2000; Petitgrand et al 2004). In the phase shifting interferometers, the measured surface has to reflect back about 15% of the light beam intensity on the surface (Blunt and Rosén 2001). As in the case of focus detection profilometers and contact profilometers the steep slopes, spheres and vertical surfaces can cause measurement problems for the interferometers. The interferometer techniques have mainly been used in areas such as microelectronics, optics, metals and crystals, where the surfaces are often smoother and have good reflection properties.

2.2.2 Scanning probe microscopy

Scanning probe microscopy is a large family of different techniques that originate from the invention of the scanning tunnelling microscope (STM) in 1981 (Binnig and Rohrer 1982). STM is usually used for high-resolution imaging not in roughness measurements, but it can also be used in roughness measurements (Krim et al. 1993; Wefers and Schollmeyer 1993). STM is based on the application of tunnelling current between a sharp tip and sample surface. This tunnelling current is the kept constant by moving the sample (or tip in some models) up and down. The height data is generated from the up and down movement of the sample, which is on the top a piezoelectric scanner. The resolution of the STM is impressive since horizontal resolution is in the angstrom range and vertical resolution in sub angstrom range. This means that STM can see single atoms on a flat surface. The limitation of STM is the need for a conductive surface since STM cannot measure non-conductive surfaces and the measurement area is small (micrometer range). Therefore, in the pharmaceutical applications where the majority of the surfaces are organic and non-conductive, STM has limited usability. STM can be used in ambient room conditions, but usually the best can be reached in vacuum conditions.

The atomic force microscope (AFM) was developed from the bases of the STM to measure non-conductive surfaces (Binnig et al. 1986). AFM is based on scanning the surface with a sharp probe, which senses the surface topography changes without an electrical current like in STM (Fig. 3). The sharp probe is part of a cantilever, which is extension of the probe. The sample (or the cantilever in some models) movement in 3D is created with a piezoelectric scanner that is one of the key element in the high resolution of the AFM and STM. AFM feedback systems tries to keep the cantilever in a similar position compared to the sample

surface by moving the sample up and down. The cantilever position is monitored with the laser diode and optical detector. The surface height data is generated from the sample up and down movement. AFM is a multitask instrument which can be used to image the surface, measure 3D roughness (profiling technique), separate different surface properties and measure force interactions.

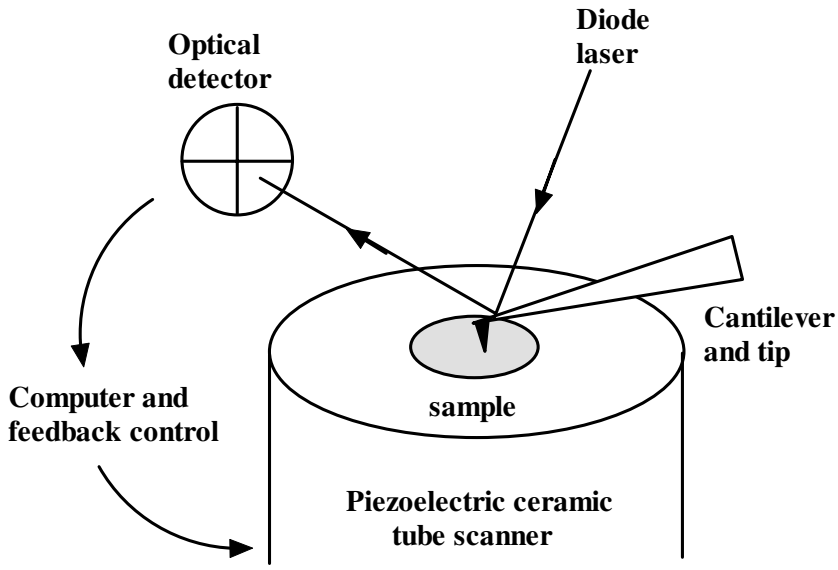

Figure 3. Schematics of AFM.

AFM measurements are commonly made in room conditions, in liquid environment (water based liquids) or in controller humidity conditions, but also vacuum AFM systems are commercially available. Commercial AFM can often measure STM, but usually in ambient room conditions. The resolution of the AFM is not quite as good as the STM resolution, but it still can reach in optimal conditions ~1 nm horizontal and sub angstrom vertical resolution. The small difference is due to less accurate probe used in a AFM. The STM can detect tunnelling current between a single atom, but the AFM senses interactions between several atoms at the time. In vertical direction, both techniques have similar resolution because the vertical resolution is governed by the measurement noise of the equipment. AFM and STM

have the same limiting factor, which is the small horizontal and vertical range. The measurement area (horizontal range) is usually maximum of 100 µm x 100 µm and the maximum vertical range is below 10 µm. AFM can measure quantitative surface roughness with extremely high resolution, but the usability of AFM in surface roughness measurements is limited due to small scanning area and low speed of the measurements. Getting a good overall view of large sample is difficult with AFM. Another limiting factor is the roughness of the surface since rough areas cannot be measured and this can have effect to roughness estimations. Surface shapes can create artefacts to the measurements because the cantilever tip (the probe) has physical shape and size. In theory, the tip cannot measure smaller surface features than its own size (tip radius 5-20 nm). In practise, AFM can reach ~1 nm horizontal resolution in special conditions when the surfaces are smooth in atomic level. For the AFM measurements problematic shapes are the same as with profilometers: spheres, vertical surfaces, deep grooves and holes Also sudden changes in surface height can causes poor surface trace of the tip, especially if the measurement speed is too high. Due to the high resolution comparison of the AFM results to other techniques is difficult because other methods cannot measure surface roughness in a same level.

The AFM has several different measurement modes that can produce a 3D image of the measured surface, provide roughness information or give information about surface properties e.g. like friction (Jalili and Laxminarayana 2004). The image produced is a computer drawn figure of the measured data (usually 512 x 512 data points). In topography images (3D surface description), the data points describe the height values measured on the surface. For this reason all the light, colour and contrast changes are computer generated from the data, meaning that AFM image is not a photograph with colours. Therefore, it is important to know about which data has been used to create the AFM image.

The most commonly used measurement techniques used to produce 3D surface images are contact mode, non-contact mode and tapping mode AFM. Contact mode AFM is the simplest measurement mode where the cantilever tip is in contact with the measured surface. In the contact mode, the tip feels the repulsive forces of the surface molecules. In addition, capillary forces from the surface contamination layer (mainly water molecules) have an effect on the cantilever tip. The capillary forces of the contamination layer create strong adhesion between the surface and cantilever tip. Due to the fairly strong interaction forces between the surface and the tip, the contact mode AFM can damage soft surfaces and create distorted images. This measurement technique is similar to the contact profilometer.

To overcome the problems with soft surfaces the non-contact AFM mode was developed (Wickramasinghe 1989). In the non-contact mode the cantilever vibrates about 50-150 Å above the sample surface sensing the attractive van der Waals forces acting between the tip and the sample (Jalili and Laxminarayana 2004). The non-contact mode is very well suited for samples with soft and sensitive samples because it does not damage the surface. Since the tip feels much weaker forces than in the contact mode the resolution is poorer. Non-contact mode AFM can produce much better resolution with suitable samples because it does not wear out the surface and measurements can be repeated several times.

Tapping mode AFM is a widely used measurement technique that combines the advantages of contact and non-contact modes (Zhong et al. 1993). In the tapping mode the cantilever is vibrated with 20-100 nm free amplitude near the surface in such a way that the cantilever tip touches the surface at the lowest point of the vibration. The tapping mode detects the long-range and short-range force interactions between the tip and surface. The tapping mode has

become the most widely used AFM measurement technique, because it can be used with all kinds of samples in different measurement environments. All the measurement modes are able produce the similar 3D surface information, which can be used to calculated surface roughness. The only main difference between the measurement modes is the usability with different kinds of samples.

AFM can be used to produce very large variety information from the surface in addition to surface topography or roughness. Quite many of these techniques require additional parts over the basic AFM. AFM can used to separate areas on the surface, which have differences in properties such as stiffness, crystallinity, chemical composition or electric properties (Wang et al. 2005; Ward et al. 2005). In addition to imaging, AFM can measure force interactions between particles and surfaces (Young et al. 2004).

2.2.3 Other methods

A confocal laser scanning microscope starts from the basis of an optical microscope, but the image is formed in a very different way (Hamilton and Wilson 1982; Aguilera and Stanley 1999). The confocal microscope can detect several different signals from the sample that are either reflected or transmitted from the sample. By varying the focal point of the optics, the confocal microscope can be used as an optical microtome. This way images from the different depths of the sample can be acquired and the information used to create a 3D image of the sample. The maximum sample depth, which can be reached, is about 40 µm. Confocal microscope has some similarity with focus detection profilometers and it can be used to measure surface roughness in a similar way (Sandoz et al. 1996; Peltonen et al. 1997).

Another profiling roughness measurement technique is light-sectioning microscopy, which can measure the surface roughness and e.g. thickness of clear polymer film (Davies et al. 1994; Twitchell et al. 1995a). In the light-sectioning microscopy the image of a slit is thrown to the surface at a 45 -degree angle and the reflection is viewed with an optical microscope at anangle of 45 degrees (Thomas 1999). If the surface is smooth, then the reflected image appears as a straight line and if the surface is rough, the line is wavy. The light-sectioning microscope has a relatively good resolution of ~0.5 µm and it can easily detect peak to valley roughness. The amount of quantitative information received by the light sectioning is limited in a similar way as with the parametric, because light sectioning does not measure profile point by point like the profilometer techniques.

The parametric roughness measurement techniques cannot measure surface profiles or produce 3D images like the profilometer techniques. The parametric methods can give statistical averages for surface peaks and valleys (Vorburger and Raja 1990). The main advantage in the parametric techniques is the speed of the measurements, which can be compared to taking photographs. The measurements take seconds not minutes or even hours like in the profiling techniques. The most common parametric methods are based on optical light scattering (Vorburger and Teague 1981; Thomas 1999). In optical light scattering, the surface is illuminated with a light beam and the reflected light is detected. If the surface were ideally flat, only one reflected beam would be detected. As roughness increases the intensity of the ideally reflected beam diminishes and a diffuse angular distribution appears. The surface roughness can be calculated from the diffuse angular distribution and the diminishing of the ideally reflected beam. Several different light scattering methods have been used to measure surface roughness, which are the specular reflectance (Smith 1999; Silvennoinen et al. 1999; Hyvärinen et al. 2000a, Hyvärinen et al. 2000b), the total integrated scatter (Rönnow

et al. 1993), angular distributions (Church 1979), ellipsometry (Vorburger and Ludema 1980) and speckle contrast (Fujii and Lit 1978). From these methods the most important are the specular reflectance and the total integrated scatter, which have been used in commercial instruments. Glossmeters are based on specular reflectance measurements and are widely used (Smith 1999). Many light scattering techniques work only with relatively smooth surfaces (< 100 nm) and therefore their usability is limited. There are also other optical roughness measurement techniques available, which are based on e.g. illumination of the surface with collimated light and analysis of the gray scale variations (Krogars et al. 2002).

2.3 Theory of surface roughness

2.3.1 The surface

A surface is a boundary that separates an object from another object, space or substance (ASME 1995). A nominal surface describes the ideal intended surface that is usually shown on a drawing or in the specifications. The difference between the nominal and the real surface is the roughness, which results from the processing of the surface. The measured surface is a representation of the real surface obtained by the measuring instrument and topography of the surface is a three-dimensional presentation of the geometric surface irregularities.

2.3.2 The real surface and roughness

The real surface is the result of several factors or flaws that are present on the processed surface (ASME 1995). The roughness is defined as the finer irregularities of the surface texture, which usually originate from the production process or material conditions of the

surface. Waviness is the wider scale component of the surface texture. The roughness may be considered as superimposed on a wavy surface. The terms roughness and surface texture are often used interchangeably because roughness is usually the one measured and specified (Song and Vorburger 1992). Roughness and waviness are included in the surface texture. Sometimes also, topography has been used with the same meaning as roughness and surface texture, but this usually does not cause a lot of confusion (Vorburger and Raja 1990). A surface lay is the predominant direction of the surface pattern and the surface texture is the composite of the certain deviations that are typical of the real surface. There are also wider deviations of the nominal surface that are not included in surface texture. These are considered as an error of form and these deviations originate from errors in the manufacturing process. Flaws are unexpected and unwanted interruptions in the topography of a surface. These interruptions are usually considered as flaws only if they are agreed to be flaws, otherwise they may be consider as part of normal topography.

2.4 The commonly used roughness parameters

A large number of different surface roughness parameters have been developed to characterize surfaces, but in this section only the more common ones are discussed.

2.4.1 Height parameters

A simplest height parameter is the peak to valley height (Rp-v) that describes the total height variation of the measured sample surface from the lowest valley to highest peak. Peak to valley information can be used for instance in evaluation of suitable roughness measurement method for certain surface, since height range (called also z range or vertical range) is

common limiting factor in roughness measurements. The problem with this parameter is the sensibility to outliers, since one exceptionally high or low height value has direct influence to this value.

The most common statistical surface height descriptors are average roughness (Ra) and the Rq (also called Rrms) roughness, which are closely related to each other (Thomas 1999). The Ra and Rq roughness parameters were defined through an electrical signal in AC voltmeter. The definition was made in a slightly different way in Europe (Ra) and in the USA (Rq). For many surfaces Ra and Rq roughness parameters can even be used interchangeably. Differences in the parameters start to show when the surface has more valleys than peaks (or vice versa), since Rq is more sensible to outliers. Ra averages out the high or low values, if their amount is small compared to the total number of measurement points. The main factors that affect the choice between Ra and Rq are the field of application and continent. The problem with Ra is that it does not discriminate surfaces with different kinds of profiles. This means that two very different surfaces (different shapes) can have the same roughness value. The average roughness (Ra) parameter is calculated from the height data according to Equation 1 (ASME 1995).

$$Ra = \sum_{n=1}^{N} \frac{\left| Z_n - \overline{Z} \right|}{N}, \qquad (1)$$

where Z_n was the individual height value of one measurement point and $\overline{Z}$ the mean value of all the height data points. N was the number of measurement points. R_a measures the average distance of the profile points to the average line (Podczeck 1997a) (Fig. 4).

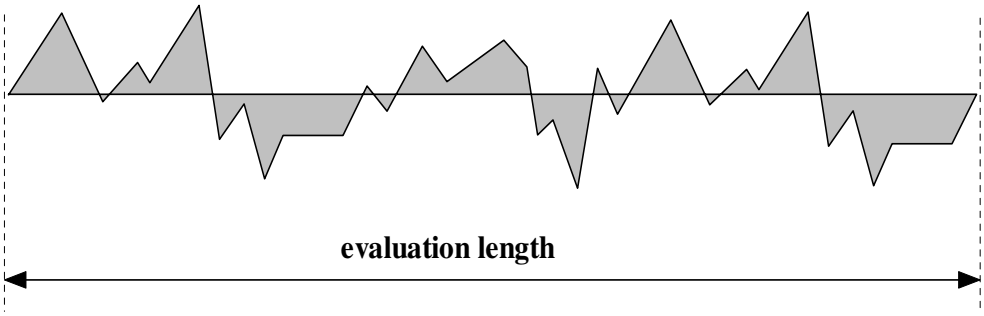

Figure 4. The average roughness, Ra measures the average distance of the profile points to the average line. In the figure Ra is the shaded area divided by the evaluation length.

The root mean square roughness (Rq) was calculated from the standard deviation of the height data according to Equation 2 (ASME 1995). Rq describes the deviation of the measurement points to the centreline and this way describes the variability of the measured profile from centreline (Podczeck 1997a).

$$Rq = \frac{\sqrt{\sum_{n=1}^{N}(Z_n - \bar{Z})^2}}{N}, \qquad (2)$$

where Ra and Rq parameters are useful estimators of the average heights and depths of surface profiles.

2.4.2 Wavelength parameters

Wavelength parameters are used to characterize the spacing of the peaks and valleys of the surface (Song and Vorburger 1992). The waviness is usually characteristic of the process that formed the surface. A typical spacing parameter is the mean spacing of profile irregularities S_m (Equation 3) that describes the mean value of spacing between the profile irregularities within the evaluation length (ASME 1995).

$$S_m = \frac{1}{N}\sum_{i=1}^{n} s_{mi}\ , \qquad (3)$$

where s_{mi} is the width of a individual peak, N number of peaks and then the mean spacing S_m is the average width of a peak over the evaluation length. S_m is usually reported in length units (µm).

2.4.3 Shape parameters

Two surfaces that have the same average roughness can have quite different shapes and therefore the surfaces can perform differently in processes (Song and Vorburger 1992, ASME 1995). There are many different shape parameters, but the most important shape parameter is the skewness, R_{sk} (Equation 4). Skewness measures the symmetry of the profile about the mean line. Surfaces with positive skewness have more high spikes on the surface and surfaces with negative skewness have more deep valleys.

$$R_{sk} = \frac{1}{NR_q^{\,3}}\sum_{n=1}^{N} r_n^{\,3}\ , \qquad (4)$$

where N number of the height values, R_q is the standard deviation of the height values and r_n is the distance between mean line and the individual height value.

2.4.4 Statistical functions

If a more complete statistical description of the surface is required, certain statistical functions can be used (Song and Vorburger 1992, ASME 1995). The most common statistical functions are power spectral density, autocovariance and autocorrelation. Power spectral density (PSD) decomposes the surface profile into its spatial Fourier component wavelengths.

Autocorrelation and autocovariance functions are widely used for visualising the degree of periodicity and randomness in surface profiles (Lysenko et al. 2001; Kiely et al. 1997; Rasigni et al. 1983; Zhang et al. 2005).

2.4.5 Fractal dimension

Fractals are continuous functions that possess the property of self-similarity (Mandelbrot 1983). Self-similarity means that they appear the same at different magnifications. These self-similar fractals can be described with a single parameter, fractal dimension D. The topological dimension of a line is 1 (Russ 2001). The fractal dimension for irregular profile is greater than 1 which is a result of the roughness. The fractal dimension for a perfectly flat surface would be 2 and the fractal dimension for real rough surfaces is larger than 2. A fractal profile function obeys a power law (Russ 1994; Mainsah et al. 2001). This means that the ideal fractal function is a straight line when plotted on a log-log scale. In practice real surfaces are not fractal over an infinite scale range. Real surfaces are the products of several different processes, which yield certain characteristic roughness. This roughness does not cover an infinite range, as an ideal fractal surface should. Real surfaces are therefore called multifractal since they have linear behaviour on a log-log plot, but there are two or more linear sections on the same plot. These discontinuity points on the plot correspond to the transition points where the process that forms the surface has changed. The fractal nature of powder systems is well established (Kaye 1993; Kaye 1995) and fractals can be used to describe quite variable systems as for example coating quality (Oliva et al. 1999) and paper surface topography (Kent 1991).

Fractal dimension is not a measure of roughness in the same sense as the roughness parameter R_a (Russ 2001). Fractal dimension does not tell us anything about the magnitude of the roughness. If we stretch the fractal surface in z (height) direction the fractal dimension does not change, but Ra and other profile based parameters increase. Fractal dimension reacts to the changes in the lateral direction on the sample surface and it is sensitive to the spatial changes of the height data. Fractal dimension can be used with different kinds of roughness analysis methods such as profilometry, scanning probe microscopy techniques and SEM image analysis (Krim et al. 1993; Chauvy et al. 1998; Li and Park 1998; Chappard et al. 2003).

2.5 Examples of surface roughness measurements

The following chapter contains literature on some examples where surface roughness measurements have been used in materials sciences. Also more specific literature about the research topics of this study is included.

2.5.1 Materials science in general

The quality of surface finish is one of the key elements in nearly all material production. Change of the surface roughness due to e.g. mechanical or chemical wear can also be an important issue. The contact (or stylus) profilometer techniques have been used especially in the roughness measurements of metal surfaces since in this case the possibility of surface damage due to stylus measurements is smaller and stylus equipment have been available longer (Chesters et al. 1991; He and Zhu 1997; Pawlus 1997; Lou et al. 2001; Le and Sutcliffe 2000; Farshad et al. 2001). In many industrial applications, the profilometer information is accurate enough for surface finish or mechanical wear evaluations. The size of the surfaces

and the measurement speed can limit use of techniques such as AFM. The AFM is better technique for research and development studies.

Surface roughness plays a part also in the research and development of soft materials. For instance printing paper surface roughness is an important property for good printing qualities and appearance of paper surface therefore the surface roughness measurements are important parameter in the paper industry (Wagberg and Johansson 1993; Rissa et al. 2000; Conceição et al. 2005; El-Sherbiny and Xiao 2005). In the printing paper, requirements for roughness can sometimes be complex because good adhesion of ink might need rougher surface than is optimal for high gloss. Similar problems can be in painting materials where high gloss is often desired property (Tiarks et al. 2003). The high gloss can be achieved with smooth paint surfaces. On the other hand, if more opacity is needed on the painted surface then the paint surface has to be rougher (Butt et al. 1995). In the soft materials optical methods are often preferred and especially if surface gloss is the parameter of interest.

Surface roughness has importance in areas, which are closer to life sciences. Dental material research has been an area where surface roughness measurements have been used extensively (Silva et al. 1998; El Feninat et al. 2001; Luo et al. 2001; Arvidsson et al. 2002; De Witte et al. 2003; Oliveira et al. 2003; Verran et al. 2003). The teeth and the teeth fillings are under heavy mechanical and chemical stress in the human mouth. Due to this reason, the roughness measurements have been used to study the mechanical and chemical wear of new dental materials or the roughness of the tooth surface. The techniques used in dental science studies have been mainly profilometer techniques, but also AFM has been used (El Feninat et al. 2001; Verran et al. 2003).

2.5.2 Crystals and powders

Crystals and powders are the key elements of solid pharmaceutical dosage forms. The powders in pharmaceuticals consist mostly from crystalline or partly crystalline particles. Several things affect the powder properties such as particle size, shape, material type and particle surface roughness. In powders particle shape and particle surface roughness can be difficult to separate since it is difficult to define where roughness ends and error of shape begins. A lot of the research done in pharmaceutics about surface roughness of powders has been connected to the force interactions between powder particles. Jones et al. have studied factors that affect powder friction (Jones et al. 2003; Jones et al. 2004). They have found that roughness is one of the important factors affecting particle-particle and particle-wall interactions. It has been shown that if surface roughness and powder particle size are in the right scale to each other the interaction is stronger (Beach et al. 2002; Jones et al. 2003; Jones et al. 2004). Surface roughness is an important factor in particle-particle and particle-surface adhesion, this has been studied extensively over the last couple of years in connection with powder inhalations (Mizes 1995; Podczeck 1997b; Heng et al. 2000; Louey et al. 2001; Sindel and Zimmermann 2001; Beach et al. 2002; Price et al. 2002; Young et al. 2003; Louey et al. 2003; Flament et al. 2004; Jiang et al. 2005). The main measurement technique in these studies has AFM, which has been used to measure the surface roughness of the surfaces, but also it has been the force measurement tool. These type studies are time consuming since the handling and measurement of powder particles is difficult. For the roughness measurements particle surface alignment for the measurement can be challenging. The effect of surface roughness on adhesion can be either increasing or decreasing, depending on the scale of particles or roughness of the surfaces (Beach et al. 2002). By modifying surface roughness of powders, the adhesion can be increased or lower that often needed in the powder inhalations.

With new particle processing techniques, the particle surface roughness can be controlled in submicrometer level (Price et al. 2002; Kaerger and Price 2004). The other processing and environmental conditions can have effect to particle surfaces. AFM is good chose in this type research since it can measure nanoscale surface roughness if the particle morphology allows it. The spherical shape and small size of nanoparticles makes the surface roughness measurements of the nanoparticles more difficult (zur Muhlen et al. 1996). AFM measurements do not usually need lot of sample preparation, but with nanoparticles the sample preparation can be critical. Nanoparticles have to be placed on a smooth substrate like smooth silicon wafer (roughness ~1 nm). The surfaces of the pure crystal faces can change while in storage this has been shown e.g. by Kiang et al. 2004. In addition, the crystallinity of the material can change which has an effect to the surface of particles (Trojak et al. 2001). This type of changes on the surfaces can be studied with imaging and roughness measurements. Imaging of surface might adequate in many cases, but 3D measurements and roughness analysis might give possibility to quantification of these changes. Fractal analysis can be combined with AFM measurements in order to analyse powder particle surface roughness (Li and Park 1998). AFM has also been used in dissolution studies of crystal surfaces where it can show the effect of dissolution as an increase in the surface roughness (Abendan and Swift 2005). Differences in surface roughness on the other hand affect the dissolution rate through the difference in surface area (Danesh et al. 2001). Another method for measuring particle surface roughness that has been used is laser profilometer, but the size of the measured particle has to be larger (<200 µm) (Poczeck 1997b; Iida et al. 2004). the contact angle of powders affects among other things wettablity of powders in granulation and on the other hand surface roughness affects the contact angle of the material (Muster and Prestidge 2002; Peltonen et al. 2004).

2.5.3 Tablets

Tablet surface roughness originates from the powder properties and tablet compression. Compression pressure during tablet compression influences the surface roughness of the compacts. Several researchers have showed this over the years (Rowe 1979; Podczeck 1998; Riippi et al. 1998; Podczeck et al. 1999a; Khan et al. 2001; Sindel and Zimmermann 2001; Eliazadeh et al. 2003). At lower compression pressures, tablet surfaces have characteristic peaks and valleys which originate from the initial powder particle morphology (Podczeck 1998; Eiliazadeh et al. 2003). At higher compression pressures, the voids between the particles close up and the surface becomes smoother. The tablets usually become smoother at high compression pressures but with a certain limit since tablets do not compress beyond zero porosity. Tablet surface roughness does not necessarily change linearly with compression pressure since sometimes there is an optimal compression pressure range where the tablets have the lowest surface roughness (Riippi et al. 1998). The type and amount of excipients also affect the surface roughness of the tablets (Peltonen et al. 1997; Podczeck 1998; Podczeck et al. 1999a; Narayan and Hancock 2003; Narayan and Hancock 2005). Brittle and ductile excipients behave differently under compression and therefore they yield different kinds of tablet surface. Generally, brittle excipients tend to produce smoother tablets than plastic excipients.

Surface roughness of tablets has been shown to have an influence on or to reflect any changes made in many process variables which have an effect on the final quality of the product. It has been shown for instance that the surface roughness of uncoated tablets has an effect on the dissolution rate of the tablets (Healy et al. 1995). Surface area is one of the key elements in dissolution. One factor influencing the tablet surface roughness is the tablet sticking to the

punches of the tabletting machine (Toyoshima et al. 1988; Roberts et al. 2003). Sticking is caused e.g. by insufficient lubricant performance, poor choice of the excipients, punch wear, high compression pressures etc. On the other hand, the surface roughness of the tablet machine punches has an effect on tabletting performance and the quality of the produced tablets (Hyvärinen et al. 2000a; Hyvärinen et al. 2000b). The surface roughness measurements can be used to describe effects formulation variables to the pellet surfaces and the structural changes of pellets induced by compression (Newton et al. 2001; Bashaiwoldu et al. 2004a; Bashaiwoldu et al. 2004b). In millimetre scale surfaces like tablets the optical methods and profilometers are at their best since they cover majority of the tablet area with one measurement. The surface height differences on the tablet surfaces are in the range of few micrometers to tens of micrometers, which limits the use of some measurement methods.

2.5.4 Coatings

There are many different types of coatings and coating materials which are used in the coatings of tablets, pellet and granules. Surface roughness is one parameter that influences the coating process and the final product quality. The surface roughness of the core tablet influences the adhesion of the film coating through the change of surface area (Nadkarni et al. 1975; Rowe 1977; Rowe 1978; Felton and McGinity 1996; Felton and McGinity 1999; Khan et al. 2001; Palasantzas and De Hosson 2003; Missaghi and Fassihi 2004). If the tablet surface is rougher, it provides larger contact area and therefore the polymer has possibility to stronger adhesion on the tablet surface (Nadkarni et al. 1975). The choice of materials, can affect the effective surface area and in this way affect the film adhesion (Khan et al. 2001). The time-dependent changes in the tablet core surface roughness also can affect the coating adhesion, but the time-dependent changes can be avoided with proper formulation and manufacturing

(Ruotsalainen et al. 2002a). In addition, materials like plasticizers can affect the surface roughness (Honary and Orafai 2003; Kwok et al. 2004). On sugar-coated tablets the roughness of lower coating layers has been shown to have an influence on the impact toughness of the coatings (Ohmori et al. 2004). The coating materials are quite often studied as free films in order to study their properties because this way the effects of the tablet core can be avoided (Lin and Meier 1995; Pérez and Lang 1999; Liu and Williams 2002; Kwok et al. 2004). In the study of free films, AFM is easier to use since free films are much smoother than the coated tablet surface. Nanometer size structures are difficult to find from surface, which has micrometer sizes height changes. The surface roughness measurements can be used to monitor the effects of different process parameters and in the quality assessment of the film coating process (Twitchell et al. 1995a; Twitchell et al. 1995b; Podczeck et al. 1999b; Krogars et al. 2002; Ruotsalainen et al. 2002a; Ruotsalainen et al. 2002b; Krogars et al. 2003; Ruotsalainen et al. 2003a; Ruotsalainen et al. 2003b). Storage can also affect the surface roughness and give signs of instability of the formulation (Ruotsalainen et al. 2003b). The surface roughness influences the outer appearance of the tablets since often a high surface gloss is required and the gloss is directly linked to the surface roughness (Rowe 1985a; Rowe 1985b; Reiland and Eber 1986; Rohera and Parikh 2002). The surface roughness of coated and un-coated pellets have also been studied (Chopra et al. 2002).

3. Experimental study design

The experimental study design of this work was following (Fig. 5). The main idea was to study surface roughness and surface imaging of different pharmaceutical surfaces of powders, tablets and coated tablets. In the beginning (I) the idea was to test different techniques on a large, relatively smooth and simple surface. The compacts of ionic powders (tablets) were chosen to be the surfaces since they form relatively smooth surface when compressed with high compression pressure. The research was continued (II) with the development of new roughness calculation and surface roughness visualisation method which was invented during the first part of the study. The tablets in I and II are named in this study as compacts to avoid mix up to the tablets and coated tablets in III. Thereafter the focus was aimed to more complex surface of coated tablets. The aim in the study (III) was to monitor the changes of the surface roughness and the development of coating film, which happens during the coating process. In the last study (IV) the focus was aimed to crystal surfaces which have more difficult micro scale surfaces. Thus, the roughness can be studied with in a wide scale from tablets to crystals.

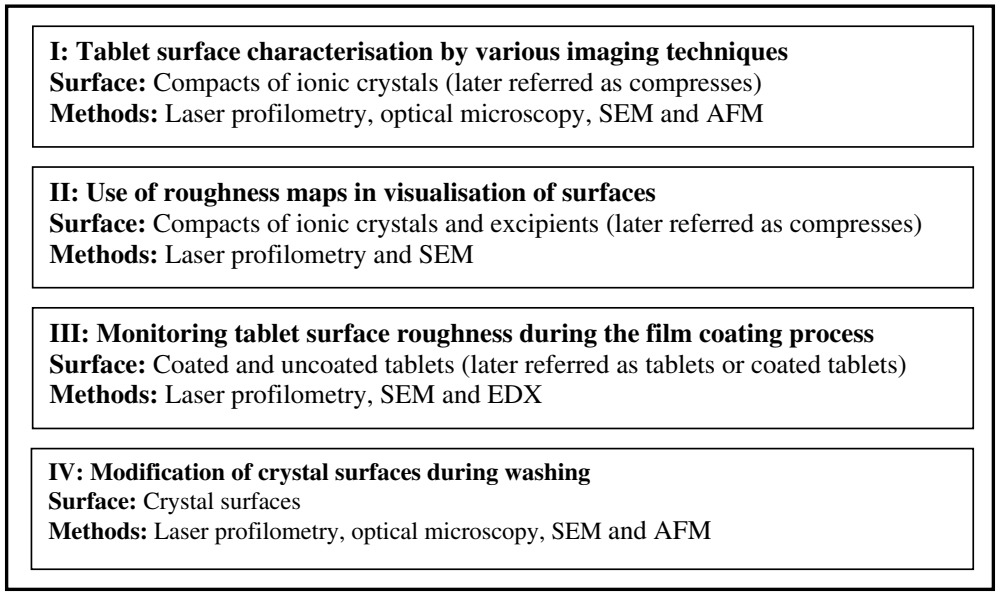

Figure 5. Experimental study design.

4. Aims of study

The overall goal of this research was to understand surface structures of pharmaceutical surfaces. In this context, the specific purpose was to compare four different analysing techniques (optical microscopy, scanning electron microscopy, laser profilometry and atomic force microscopy) in various pharmaceutical applications where the surfaces have different scale of roughness. The specific aims were:

1. To compare the image and roughness analysing techniques using model surfaces, which were tablet surfaces (compacts of powders compressed by IR press) compressed with high compression pressure.

2. To develop a new method which can give information on the localised roughness across a wider area and build up the easily readable roughness maps of the surfaces.

3. To evaluate the change of surface roughness and the development of the coating during the film coating process using laser profilometer roughness measurements, SEM imaging and EDX analysis.

4. To characterise the changes in the crystal surface caused by washing.

5. Experimental

5.1 Materials

Test materials in the studies of powder compact surfaces were analytical-grade sodium chloride (NaCl) (Riedel-de Haën, Seelze, Germany) (I-II), potassium chloride (KCl) (Riedel-de Haën, Seelze, Germany) (I-II), M325 lactose monohydrate (DMV international, Veghel, Netherlands) (II) and Ph. Eur. grade of theophylline anhydrate (BASF, Ludvigshafen, Germany) (II).

In the tablet coating study (III) the following materials were used for preparing tablet cores: theophylline anhydrate (Ph.Eur.), microcrystalline cellulose (Avicel PH-102, FMC International, Little Island, Cork, Ireland), talc (Ph.Eur.) and magnesium stearate (Ph.Eur.). The composition of the tablet cores was as follows: theophylline anhydrate 5% (w/w), microcrystalline cellulose 86% (w/w), talc 8% (w/w) and magnesium stearate 1% (w/w). The two aqueous film coating solutions contained: (1) 8% (w/w) hydroxypropyl methylcellulose, HPMC (Methocel E5, Dow Chemical, Midland, MI, USA.), 1.6% (w/w) polyethylene glycol, PEG 400 (Macrogolum 400, Fluka Chemie, Buchs, Switzerland), purified water 90.4% (w/w) (Ph.Eur.) and (2) titanium dioxide 2.4% (w/w) (Ph.Eur), 8% (w/w) hydroxypropyl methylcellulose, 1.6% (w/w) polyethylene glycol and purified water 88% (w/w).

The water used in the crystal washing (IV) was purified water and the glycine powder was α-glycine (Glycine minimum 99% TLC, Sigma-Aldrich Chemie, Steinheim, Germany). The ethanol used in the crystallization and in the washing was AA grade (99.5 %).

5.2 Processing equipment and methods

5.2.1 Compression of powder compacts

The powder compacts (I-II) were compressed with a 13 mm evacuable IR tablet die (Specac Ltd., Orpington, United Kingdom) and a hydraulic press (Pye Unicam, Cambridge, United Kingdom). The compression forces were 30 kN and 80 kN and the compression time was two minutes. Corresponding compression pressures were 225 MPa and 600 MPa. The high compression pressure (600 MPa) was used to produce as smooth a compact surface as possible. The lower compression pressure (225 MPa) was used as a reference. The tablet die was evacuated by a vacuum pump during the compression. The compact weight varied between 300 and 450 mg. Prepared compacts were attached to metal sample plates with double sided tape in order to assist in the handling and identification of the correct compact surface.

5.2.2 Preparation of tablet cores

The tablet cores for coating (III) were compressed in a rotating tablet machine (Kilian & Co., GmbH, Köln, Germany) to a constant breaking strength of 95-100 N using 11-mm biconcave punches. The average weight of the tablets was 500 mg and their friability was 0.6%.

5.2.3 Preparation of coating solution

The preparation of the coating solution and pigment dispersion was made as follows. Half of the calculated amount of water was heated (80-90 °C) and the polymer was added to the hot water under magnetic stirring. After the polymer had been dispersed, the remaining cold water

was added. When all the polymer was dissolved, the plasticizer and the pigment were added to obtain a total of 1000 g of coating liquid.

5.2.4 Film coating of tablets

The tablets (III) were film coated in a laboratory-scale instrumented side-vented drum-coating apparatus (Thai coater, model 15, Pharmaceuticals and Medical Supply Ltd Partnership, Bangkok, Thailand). Each coating batch comprised of 1.0 kg tablet cores. In the film coating experiments, the conditions of user-controllable process parameters were adjusted as follows: pump speed (flow rate) 2.8 rpm, pneumatic spraying pressure 300 kPa, drum air temperature 40°C, rotating speed of the drum 7.0 rpm, air pressure (drum) -5.0 Pa and outlet air flow rate 20 l/s. The tablets were pre-heated for 5 minutes until the drum temperature was 40°C, and the rotating speed of the drum was adjusted to 3.0 rpm for the pre-heating and post-drying steps. After spraying, the tablets were dried for 5 minutes at 40°C in the drum-coater. Thereafter, the film-coated tablets were kept at a controlled room temperature (25°C/RH 60%) for at least 24 hours until they were studied. During the film coating multiple samples of the film-coated tablets (n = 20-30) were taken immediately prior to film coating (the spraying phase) and subsequently at 2.5, 5, 10, 15, 20, 30 and 45 min. The timing for the samples started at beginning of the spraying phase. The end point (the final coated tablets) were covered after 60 minutes of process time which consisted of 55 minutes of spraying and 5 minutes of end drying.

5.2.5 Vapour diffusion crystallization of glycine

Glycine-water-solutions (IV) were prepared at two different concentrations (A= 18 g/100 ml; B= 28 g/100 ml). The water used was purified water and the glycine powder was α-glycine.

Nine 50 ml beakers of glycine-water solution were placed in a closed chamber with 500 ml of ethanol (AA grade, 99.5%). As it is a more volatile solvent, ethanol will transfer into the water solutions via vapor diffusion. Ethanol was used as an antisolvent and hence it causes glycine to crystallize. Vapor diffusion induces slow crystal growth and therefore the crystals formed are of high quality. The crystals were grown in this study for about 3-4 days.

5.2.6 Cleaving and washing of the crystals

The best quality crystals came from solutions of 28 g/100 ml concentration which produced large and clear crystals. All the crystals used had the same basic crystal shape, but there were large size variations between the crystals. The largest crystals were chosen for cleaving since the aim was to have at least 1 mm wide slices for the laser profilometer. The cleaved crystal slices were about 1-2 mm wide and about 10-20 mm long (IV, Fig. 1a). The cleaving of the α glycine (GLYCIN02) crystals were done with a surgical knife and the cleaving was done along the [010] slip plane of the crystals. The cleaved crystal slices were about 1-2 mm wide and about 10-20 mm long. The theoretical step height into the direction of the [010] plane is 8.9Å which is the height of a single bilayer (Marsh 1958; Carter et al. 1994).

The cleaved crystal slices were washed either with purified water or ethanol. One drop of water or ethanol was dropped on the crystal surfaces with a microsyringe and spread on the crystal surface. The volume of the ethanol droplet was 8 µl and water 13 µl. The surface was left to dry in air at least for 30 minutes before any measurements were made.

5.3 Analysing equipment and methods

5.3.1 Image, surface imaging, surface characterisation and image characterisation

The term “image” in this study was used in the context of the optical microscope, the scanning electron microscope (SEM), laser profilometer and atomic force microscope (AFM) images. From “images” only the optical microscope images were direct visual images of the physical surface. The images from other techniques were computer calculated visualisations of the measurement data. The term “surface imaging” has been used to describe to the use of different image producing techniques (mentioned in the first sentence) in the visualisation of the studied surfaces. “Surface characterisation” has been used to describe use of imaging and roughness techniques in the description of the surface structure and surface roughness.

5.3.2 Particle size of the powders

The particle sizes and morphology of the NaCl and KCl were evaluated by scanning electron microscopy (SEM) (see below) (I). Both test materials had a particle size around 250 µm (I, Fig. 1a – 1b). NaCl particles had an obvious clear cubic crystal habit, whereas KCl particles were more irregular. The particle size of the powders (II) was also determined with a Leica MZ-6 optical microscope (Leica DMLB, Leica Microskopie & Systeme GmbH, Wetzlar, Germany) which was equipped with Leica QWin image-analysis software (Leica QWin V2.6, Leica DMLB, Leica Microskopie & Systeme GmbH, Wetzlar, Germany). At least 800 particles were used in each particle size determination by measuring the horizontal and the vertical dimensions from which the averages were calculated.

5.3.3 Glycine structure

The α-glycine powder (IV) used was α-glycine characterized by XRPD (Bruker AXS D8, Bruker AXS GmbH, Karlsruhe, Germany). The [010] slip plane on the crystal slice surface was also confirmed by XRPD analysis. The crystal structure of the α-glycine was visualized by Mercury software (The Cambridge Crystallographic Data Centre, Cambridge, UK).

5.3.4 Glycine contact angle

The contact angles between the glycine surface and the solvents were measured with a contact angle measurements system (CAM 200 Optical Contact Angle Meter, KSV Instruments Ltd, Helsinki, Finland).

5.3.5 The thickness of the tablet film coating

The thickness of the coating (III) (35-40 µm) was estimated from the increase of the tablet height (n=10), which was measured with a digital micrometer (Sony Micrometer, Sony Magnescale Inc, Tokyo, Japan).

5.3.6 Optical microscopy and scanning electron microscopy

The overall view of the tablet surfaces was taken with an optical microscope (I) (Leica DMLB, Leica Microskopie & Systeme GmbH, Wetzlar, Germany) and a Scanning electron microscope (SEM) (I-II) (Zeiss DSM 962, Oberkochen, Germany). The SEM pictures were also used as a reference for the laser profilometer measurements (I-II). The magnifications used x200 lactose monohydrate and x500 for theophylline anhydrate powders were (II).

The surface of the film-coated tablets (III) was also studied by SEM. The preparation of the sample was accomplished by placing the tablet on the specimen holder. The samples were coated with a gold-palladium target using a vacuum evaporator. SEMs were obtained at an acceleration voltage of 8-10 kV. Energy dispersive X-ray analysis (III) (EDX) as an extension of the SEM (Oxford Isis EDS-detector, Oxford Instruments Ltd., High Wycombe, United Kingdom) was used to detect the magnesium stearate and titanium dioxide of the tablets. EDX analysis was used in the mode of semi-quantitative detection and the acceleration voltage used was 20 kV. The magnification used during the EDX analysis was x50.

In the study IV the crystals surfaces were imaged by the built in optical microscope (with 20 x optical lens) of the atomic force microscope (Autoprobe CP, Thermomicroscopes, Sunnyvale, CA, USA) in order to give general view of the crystal surface.

5.3.7 Laser profilometry

Millimetre scale areas of the powder compact surfaces were measured by a laser profilometer (UBM Microfocus Measurement System, UBM Messtechnik GMbH, Ettlingen, Germany), which was used to image and measure the roughness of the compact surfaces using image sizes 1 x 1 mm (I) and 2 x 2 mm (I-II). The measurement range was ± 50 µm, the laser spot size was 1 µm and the lateral resolution was 1000 points/mm. The resolution in the vertical direction was ± 0.1 µm. The laser output was 0.2 mW and the laser wavelength 780 nm. Roughness parameters average roughness (Ra) (I-II), the root mean square roughness (Rq) (I-II) and the peak to valley height (Rp-v) (I) were calculated from the 1 x 1 mm (I) or 2 x 2 mm (II) measurement areas. 3D images were drawn from 2 x 2 mm data files using Mathematica 4.0 software (Wolfram Research Inc, Champaign, Illinois, USA). After data collection the

image data was levelled to remove the slope caused by the tilting of the tablet surface and tilting caused by the sample plate and double-sided tape using a data-analysis program (Ubsoft version 2.8 DOS, UBM Messtechnik GMbH, Ettlingen, Germany).

The surface roughness of the tablet cores and the coated tablets (III) were also measured with the same laser profilometer. In this study, the surface roughness was studied using an area of 3 mm x 3 mm and a lateral resolution of 125 points/mm. The measurement time for each tablet was 30 minutes. The average roughness values (Ra) were determined from at least six tablets. After data collection, the image data was levelled to remove roundness caused by the roundness of the tablet using the Ubsoft data-analysis program. At the same time as the roughness information, the reflectance signal from the laser profilometer was also recorded. The maximum reflectance of 100% corresponds to a mirror surface and 5% is the minimum reliable reflectance of which measurement can be made. The tablet core surfaces and the final coated tablet surfaces were also measured with a higher resolution of 1000 points/mm, in order to image the 3D shape of the surface. Laser profilometer images showing the 3D shape of the surface were drawn by the Mathematica 4.0 program as mentioned above. The differences in the results were analyzed using Student's t-test in Microsoft Excel software (Microsoft Excel 2002, Microsoft Corporation, Redmond, WA, USA).

The same laser profilometer was used to measure the surface area of glycine crystals on a larger scale (IV). The surface roughness was measured from a 1 mm x 3 mm area, but the actual calculation of the roughness values was made from a 0.5 mm x 1.5 mm area to remove the problems caused by crystal slice edges in some crystals. The roughness parameter used in this study was of average roughness (Ra). All the crystal slices were positioned in the same

direction during AFM and laser profilometer measurements. The longer axis of the crystal slice was always parallel to the horizontal direction of the images.

5.3.8 Atomic force microscopy

Atomic force microscope (AFM) (Autoprobe CP, Thermomicroscopes, Sunnyvale, CA, USA) was used to image the microstructure of the compacts and crystal surfaces from 10 µm x 10 µm (I), 50 µm x 50 µm (IV) and 90 µm x 90 µm (I) areas. The measurements were made using 512 x 512 point measurement density. The surface roughness values were calculated from 90 µm x 90 µm areas (I). AFM imaging was performed in the tapping mode (I and IV) with a cantilever which had a spring constant of 3.0 N/m (Silicon cantilever NSCH11A, NT-MDT Ltd, Moskow, Russia). In addition, contact mode imaging was used with some crystal samples (IV). AFM imaging was carried out in normal room conditions using a large area scanner (100 µm lateral scan size).

5.3.9 Calculation of roughness maps

The roughness parameters (II) Ra and Rq were calculated in two different ways from the laser profilometer data: first by the Standard method using the analysis program submitted with the equipment Ubsoft software (see above) and then by our new Matrix method, which gives detailed localized roughness information about the surface. The standard method gave a single roughness value for both the Ra and Rq parameters describing the whole measured 2 x 2 mm area.

In the new Matrix method (II) the 2 x 2 mm areas (corresponding to 4 million data points) were divided into 400 small squares (squared matrixes) and the Ra and Rq roughness parameters of those squared matrixes were calculated using Mathematica 4.0 (II, Fig. 1). The size of the squares was chosen to be 10000 points in order to achieve adequate statistical significance for the local surface roughness estimates. A similar division of the measured area into smaller sections was earlier described in the literature by Yoshinobu et al. (Yoshinobu et al. 1994), but they used the sectioning for the measurement of scale independent roughness from atomic force microscope images. In this study, the Ra roughness values of the small squares were drawn to roughness maps which illustrate the variation of the roughness on the different areas of the sample surface. The roughness values in the roughness maps were scaled between 0 and 1 to enhance differences in the maps. The roughness maps were used to condense the large amount of information in the original laser profilometer images. By this way, the roughness maps help to visualise differences in local roughness.

6. Results and discussion

The following chapter is divided so that in the sections 6.1 – 6.3 are concerned with the surfaces describing through different imaging techniques and in sections 6.4 – 6.6 the surfaces are described through roughness measurements.

6.1 Surface imaging by optical microscopy and scanning electron microscopy

6.1.1 The surfaces of the powder compacts

In the studies of model compact surfaces (I-II) made from potassium chloride, sodium chloride, lactose and theophylline the microscopy results suggested that for all the materials the lower 30 kN compression force yielded rougher compacts than the compacts made with 80 kN compression force. This supports the earlier findings with other excipients that a higher compression force usually produces smoother tablets (Rowe 1979, Podczeck 1998, Riippi et al. 1998; Narayan and Hancook 2003). Even though the compression pressures in used this study where higher (225 and 600 MPa) than those in the used in the previous studies (mostly <150 MPa). Optical microscopy and SEM (I) showed that the general appearance of the KCl compacts were smoother than the NaCl compacts and the smoothest compact was the 80 kN KCl compact (I, Fig. 2a and 3a). This is most likely due to the difference between the melting points of the ionic powders (NaCl 801 °C, KCl 776 °C) and the differences in the atomic radiuses of the sodium and potassium, since the particle sizes of the powders were similar (~250 µm). Also, SEM images (II) suggested that with lactose monohydrate and theophylline anhydrate, higher compression pressure produced surfaces where holes or gaps between particles were smaller because the higher compression pressure packed the particles closer to each other (II, Fig. 2a-2d). A similar phenomenon was also seen with the KCl and NaCl

compacts (II). The smaller holes between particles yield smaller roughness this has been shown also by Narayan and Hancook (Narayan and Hancook 2003).

The particle size and shape of the original test materials were still visible in the optical microscope (I) and SEM images (I-II) of the compact surfaces (I, Fig. 2 a – 2d and 3a – 3d; II, Fig. 2 a – 2d). NaCl and KCl had a particle size around 250 µm according to the SEM images (I, Fig. 1a – 1b). The particle sizes of KCl, NaCl, lactose monohydrate and theophylline anhydrate were also studied by image analysis (II, Table 1). There were not large differences in the particle sizes of the ionic materials between the SEM images (~250 µm) and the optical image analysis (KCl 190 ± 92 µm, NaCl 210 ± 130µm) results. The large particles of KCl and NaCl (I) were easier to identify from compact surfaces than the smaller organic particles (II) (average sizes 30-40 µm). Especially in the case of the NaCl compacts (I), the characteristic cubic particles were clearly detectable, since the particles were not joined together as uniformly as in the KCl compacts. With the organic materials (II) the original particle borders were easier to identify in the case of lactose monohydrate compacts, but the original "crystals" were also visible in the theophylline anhydrate compacts. With the lower compression pressure, there were a number of small particles (<10 µm) visible on the surface of the lactose monohydrate compacts. This could not be seen on the compacts made with the higher compression pressure. On the 80 kN lactose monohydrate and theophylline anhydrate compacts the holes between larger particles (tens of micrometers) seemed to be filled up with smaller particles. This suggested that fragmentation is the main compaction phenomenon which created smoother surfaces. Lactose monohydrate has been described to compress mainly with fragmentation, which can lead to the formation of small particles filling the holes between larger particles (Roberts and Rowe 1986; Bolhuis and Chowhan 1996; Narayan and Hancook 2003). On the other hand, theophylline anhydrate has been described to compress

with a plastic flow at compression pressures below 150 MPa (Suihko et al. 2001). It is evident that with the higher compression pressures (225 and 600 MPa) used in this study, theophylline anhydrate particles fragment that might explain the smaller particles seen in the 80 kN theophylline anhydrate compacts.

Optical microscopy and SEM are good techniques for the assessment of the roughness and quality of the tablet (compact) surfaces. Just by looking the image information, it can be difficult to give accurate descriptions of the roughness differences between samples if the roughness differences are small. For a fast overall classification of tablet surface roughness, optical microscope is the better method than SEM because it is faster and cheaper. The advantage of the SEM is the higher resolution. The effect of compression pressure to the surface roughness has been studied earlier with different excipients and different compression pressures. This gave a good background for studying the use of imaging and roughness analysing techniques and their usability, even though the surface roughness does not necessarily degrease linearly with the increasing compression pressure as e.g. Riippi et al. have shown (Riippi et al. 1998).

6.1.2 Monitoring the tablet coating process

On the tablet core surface (III) the particles of microcrystalline cellulose were easily seen in the SEM images (long particles, 50-100 µm in length) (Fig. 6). The surface had flat areas, which were formed from one large particle or several smaller particles. Between flat areas there were deep and wide holes, some being ~20 µm in diameter. When the spraying time in the batch without the pigment had lasted 2.5 minutes, some slight modification and coating of the surface could be seen in the SEM images, but the surface was nearly the same as that of the core tablet (Fig. 6). After 5 minutes coating, there were areas on the tablet surface that had

coating, but most of the surface still had the appearance of the core tablet (Fig. 6). After 15 minutes the surface had been fully covered with a thin coating layer and only larger holes from the tablet core were visible under the coating (Fig. 6). After 30 minutes, the coated surface did not change markedly (Fig. 6). The development of the coating batch with titanium dioxide was similar as the batch without the pigment, but there were small particles visible in the pigmented coating (Fig. 6). These particles were titanium dioxide aggregates.

The SEM images give a good general view of the development of the tablet coating. The problem with the SEM imaging of the large coated tablets is slowness of the vacuum development during the measurements. This limits the number of samples. This is due to the air and the moisture that is trapped inside the tablets and is released during the vacuum pumping. In addition, there is a risk of melting or burning the polymer film on the tablet surface with the electron beam. The optical microscope would faster choice, but problems with optical microscopy are the resolution and the image contrast on a white surface.

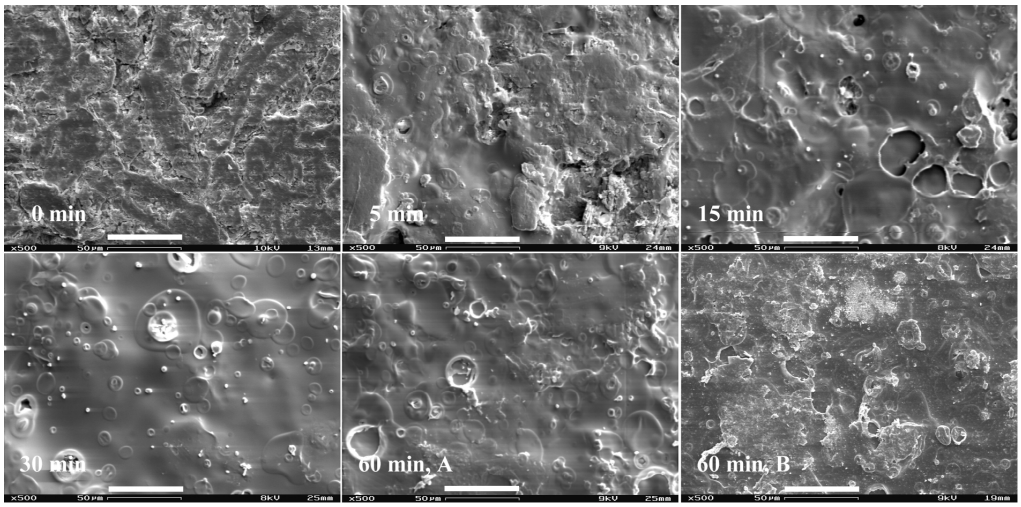

Figure 6. Scanning electron micrographs (SEM) showing the progress of film coating of tablets in a side-vented drum coater. Key: 0 min (surface of the tablet core), 5 min (batch unpigmented), 15 min, 30 min, 60 min, A (final unpigmented film-coated tablet batch) and 60 min, B (final pigmented film-coated tablet). Magnification x500, length of scale bar 50 µm.

The EDX analysis option of the SEM was used in order to get additional information about the polymer coating coverage on the tablet surface at different time points during the coating. The EDX analysis of tablet cores (III) clearly showed a magnesium peak which came from the magnesium stearate of the tablet formulation (III, Fig. 4). The magnesium signal in the EDX spectrum was clearly seen in the core of the tablet, and the samples taken at 2.5 minutes and 5 minutes (III, Fig 4 and 5). In the 15 minute sample, the magnesium signal was clearly weaker than in the earlier samples. The 30-minute sample and subsequent samples did not have a magnesium signal in the EDX spectrum. It was observed that after 15 minutes of coating, the polymer film covered the tablet surface almost completely and after 30 minutes the film covered the whole surface. In batch 2, the magnesium signal was still visible after 2.5 and 5 minutes, but after 15 minutes of spraying the peak was not visible. The titanium peak was strong after 2.5 minutes of spraying and was at a similar level after 5 minutes (III, Fig. 5). After 15 minutes, the signal became stronger and at later time points the signal strength did not change remarkably. The EDX analysis was done with small magnification (x50 versus x500) than the SEM imaging in order to get information on a larger area than the shown SEM images cover (Fig. 6). With this smaller magnification approximately 2 mm x 2mm area was covered. The samples were coated with a gold-palladium target, but other option could have been carbon coating using a vacuum evaporator. The carbon coating might have given a better signal strength in the EDX, but negative side would have been poorer image quality in the SEM images. EDX analysis gives valuable information about the basic elements on the tablet surfaces, but usually due to measurement time limitations only a limited number of samples can be measured as in the case of SEM.

6.1.3 The crystal surfaces

The optical microscopy was able to visualise some of the largest features (crystal steps) of the crystal surfaces (IV) and gave a quick general comprehension of the whole crystal surface. The optical microscope showed large differences in the step density on the pure glycine slice surfaces (IV, Fig. 3). In some areas there were several crystal steps (visible by optical microscope) in within 100 µm distance and in others one or no steps at all. The step density differences could be seen not only in the optical microscopy and laser profilometry images, but also in the AFM images on a different scale (IV, Fig. 2 - 4). The steps and other surface features seen on the crystal surface were most likely due to the cleaving of the crystals (Swain et al. 1974; Sangwal et al. 1997; Shindo et al. 2001; Borg and Sangwal 2004). The optical microscope images showed similar larger scale crystal steps on the pure crystal surface as the laser profilometer. Typically, these steps were seen as parallel lines in the images. The reason why the step density differences appear is the in the crystal defects and how the cleaving affect to them. In optimal case the crystal would cleave along the same crystal plain leaving no steps.

Ethanol washing changed the surface of the crystal slightly on a larger scale, but the largest crystal steps were still recognisable by the optical microscope, only some of the smaller crystal steps had disappeared (IV, Fig. 3). The water washing cleared all recognizable surface features from the surface and the size of the whole crystal diminished slightly. The water washed surface looked smoother under the optical microscope since there were no large crystal steps that could be seen, but in reality, the surface clearly became rougher after the water washing. The optical instruments have a theoretical maximum resolution of 1 µm, and thus we cannot see the small scale changes on the crystal surface with them. On the other

hand, the optical methods can cover the whole crystal surface at one time to give a statistically relevant picture of the whole crystal.

6.2 Surface imaging by Laser profilometer

6.2.1 The powder compact surfaces

Laser profilometer images were used in the characterisation of compact surfaces made by an IR press (I-II). Many compact surface features visible in the optical microscopy images were also visible in laser profilometer images (I, Fig. 4). The original KCl and NaCl powder particles (size ~250 μm) were easy to recognize from the images. The original organic powder particles were nearly visible in the laser profilometer images (II, Fig. 3 and 4). The laser profilometer images also showed that higher compression pressure produces smoother surfaces because the particles were packed denser (Podczeck 1998; Riippi et al.1998). Laser profilometer images support the findings of optical microscopy (I) and the SEM (II) as described above. Especially with lactose monohydrate (II), both size and amount of holes or gaps between the larger particles were smaller with the higher compression pressure. Similar behaviour was also observed with KCl and NaCl (I). The laser profilometer showed that the "particle" areas on the NaCl and KCl compacts were not at the same height level (Fig. 7). This can be seen as a colour difference in the figure between neighbouring particles. Most likely this means that compression pressure has not divided equally on the tablet as the Eiliazadeh et al. have shown earlier (Eiliazadeh et al. 2003). The relaxation of the tablet structure after compression has ended might also have influenced to the surface height differences. There were some small areas on the 30 kN NaCl compacts, which were not properly imaged by the laser profilometer. These image defect areas existed in the particle

border areas, next to some large holes. The image defects were caused by poor laser beam reflection from the compact surface, a problem that affects the height data and thus the reliability of the data. The laser profilometer can produce images from the surface that have similar resolution on the horizontal plain as the optical microscope. Optical microscopy is of course much faster technique in imaging than the laser profilometry, but it lacks the height scale information of the profilometer. From the laser profilometer images it is possible to see how for instance the powder particles have joined since the images are drawn from the height information.

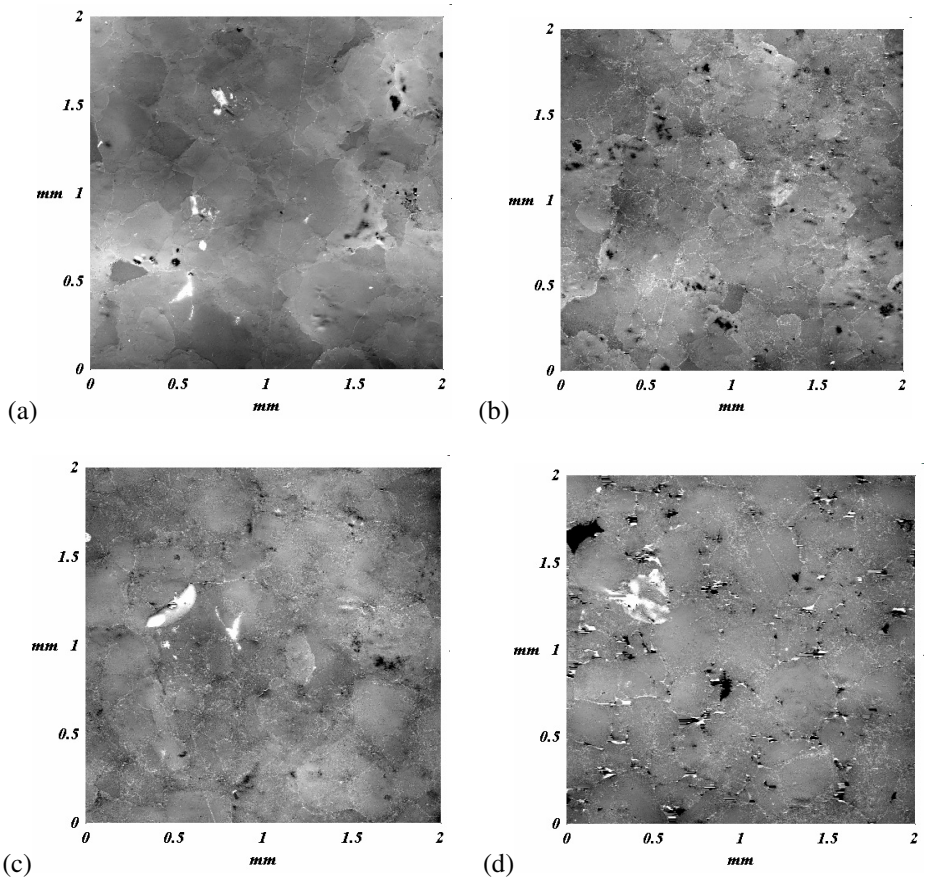

Figure 7. Laser profilometer micrographs of the compacts (I) (a) 80 kN KCl, (b) 30 kN KCl, (c) 80 kN NaCl and (d) 30 kN NaCl.

6.2.2 The monitoring the tablet coating process

On the tablet core surface (III) the particles of microcrystalline cellulose and deep holes were seen in the SEM images as mentioned above (Fig. 6). The laser profilometer images also showed flat areas and that there were deep holes on the tablet core surface (III, Fig 2a) The laser profilometer images from the coated tablets look quite different when compared to each other (III, Fig. 2b and 2c). The surfaces of tablet without pigment surfaces looked rougher and more porous in the laser profilometer images. The surface shapes without the pigment seemed to be sharper. The surface of the tablet with pigment had a slightly smoother appearance and had rounder shapes on the surface. It occurs due to the better reflection properties of the batch 2 coating caused by the titanium dioxide. The reflectance signals from the profilometer recorded at the same time as the roughness measurements were made showed that the batch with pigment had clearly better reflection properties (27%) than the batch or the core tablets (III, Fig. 3). The core tablets had reflectance of 19%, which was higher than the value of the tablets from the batch without the pigment (14%). During the film coating process the amount of reflectance changed differently in the batches with or without the pigment. In the un-pigmented batch, the reflectance started to decrease right from the beginning and continued decreasing for 45 minutes. The reflectance value decreased from 19% to 14%. After 45 minutes of spraying, the reflectance remained at the same level. In the pigmented batch, the reflectance did not change at the beginning but then the reflectance started to rise for 45 minutes, at which point the reflectance reached its maximum (~27%). The reflectance information has to used carefully since surface roughness also affects the amount reflection, not only the material reflection properties. In this study, there were not clear roughness differences between the batches, so the effect of the roughness to the reflection should be irrelevant. Laser profilometer reflectance information has previously been used to give

qualitative information about the surface properties of tablets and about surfaces containing pigments (Salako et al. 1998; Rissa and Lepistö 2000).

6.2.3 The crystal surfaces

On the crystal surfaces (IV), the laser profilometer images revealed differences in the density of the crystal steps (IV, Fig. 4). The step density differences were also seen in the optical microscope and AFM images, but on a different scale. As described above the mechanical stress caused by the cleaving was the most likely reason for the crystals steps seen on the glycine crystal surfaces. According to the laser profilometer measurements, these steps were in the order of dozens of molecule layers thick and the distance between the steps were from tens of micrometers to hundreds of micrometers. On a typical pure glycine surface the steps were roughly 50 nanometres high, corresponding to about 50 molecule layers. After ethanol, washing the same surface looked slightly different. The small steps had disappeared and they were replaced by a couple of large crystal steps (height about 150 nanometres). At some places on the pure glycine surface there were some small crystal fragments which came from the cleaving process (IV, Fig. 4c). Water washing cleared all the previous surface features and the remaining surface was much rougher than before the washing or after ethanol washing.

Glycine is poorly soluble in ethanol and ethanol evaporates much faster than water, this explains the small effect to the surface. Earlier Wen et al. had shown that many organic solvents have a very small effect on the surface of the α-glycine crystals (Wen et al. 2004). In addition, the volume of the ethanol droplet was about half of the water droplet. These factors support the results from the laser profilometer measurements that indicate that ethanol washing had an insignificant (± 10%) effect on the surface roughness of glycine surface.

The laser profilometer gives better image of surface height differences on the crystal surfaces than optical microscope. From the optical microscope, images it can difficult to estimate for instance which of the crystal steps is higher or lower compared to the next step. Again, the imaging by laser profilometer is slow and horizontal resolution is not better than the resolution of the optical microscope. In the laser profilometer and AFM, images the height scale differences between different images can cause some confusion because the colour scale of an image is set according to the height range the measurement data. This means that the height scales can be difficult to estimate without any numerical height data (roughness data). The due to colour scaling limitations it is difficult to see smaller structures in the image if there are large height differences. For instance the step structure on upper part of the figure 4c (IV) is similar to the step structure in figure 4a (IV). In the figure 4c the structure is seen poorly due to different kind of colour scale, which originates from one large step in the lower part of the image.

6.3 Surface imaging by AFM

6.3.1 The powder compact surfaces

Too high surface roughness is the largest limiting factor in AFM imaging. Usually, all tablets have areas on the surface, which are too rough to measure or local roughness limits the proper image size markedly. For example, the tablets and coated tablets in the coating study (III) were too rough for reasonable AFM analysis. That is why the AFM imaging of the KCl and NaCl compacts (I) was done on a chosen flat area in order to get as big an image as possible. The best areas to image were the faces of the large “particles”, meaning places where the original powder particles were recognisable. In the case of the 30kN and 80 kN KCl compacts

borders between particles were smoother in the NaCl compacts. Increasing compression pressure made the KCl and NaCl compacts smoother and less porous (I, Fig. 5). The characterisation of tablet surfaces by AFM has not been widely discussed in the literature but it has been shown that increasing compression pressure could yield smoother tablet surfaces (Sindel and Zimmermann 2001; Muster and Prestige 2002). Surface features on the 80 kN KCl compacts were very smooth and had a round shapes but the surface shapes of the 30 kN compacts were much sharper and the surfaces were much rougher. The situation with NaCl compacts seemed to be quite similar to the KCl compacts. According to the literature in the case of NaCl there is a decrease in porosity between 225 MPa and 600 MPa compression pressures (compression forces 30 kN and 80 kN) (Adolfsson and Nyström 1996). With 600 MPa compression pressure (80 kN compression force) NaCl is very close to the zero porosity. The 80 kN NaCl compact was smoother and its surface was full of a layer structure which might be due to recrystallisation of the NaCl. The NaCl compacts made with a lower compression pressure they also had large cracks on its surface that reflect the greater roughness and porosity. The AFM is good technique to image the tablet surfaces in special cases when especially high resolution is needed in combination to a need of quantitative information from the surface. By the AFM is it possible to measure distances and height differences in addition to the roughness parameters. The AFM is not a good choice when good statistical coverage of the surface is needed.

6.3.2 The crystal surfaces

In the imaging of the crystal surfaces (IV) AFM was able show large differences in the step density on the pure glycine slice surfaces (Fig. 8 and IV, Fig. 2). The step density differences could be seen not only in the optical microscopy and laser profilometry images, but also in the

AFM images. The step density in the AFM images ranged from a very dense structure where the steps where less than 1 µm apart from each other to areas where the steps were tens of microns apart. Similar differences were seen in the larger scale images taken by an optical microscope and laser profilometer.

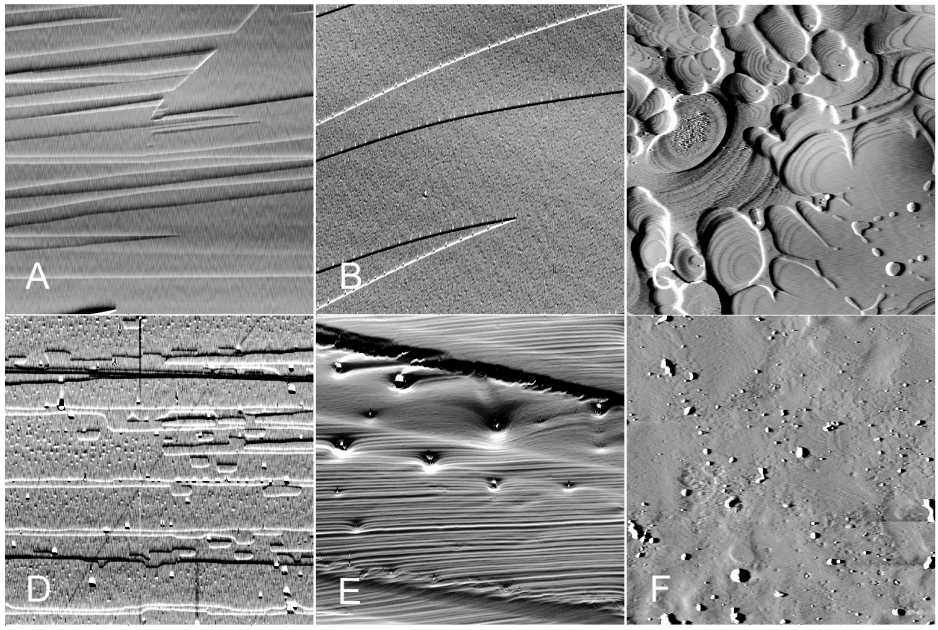

Figure 8. AFM image of the glycine crystal surface, 50 µm x 50 µm. a) Pure cleaved surface of glycine crystal, Ra roughness 0.52 nm. b) Pure cleaved surface of glycine crystal, Ra roughness 0.28 nm. c) Ethanol washed surface of the glycine crystal from the same area on the surface as in Fig. 5a, Ra roughness 4.60 nm. d) Ethanol washed surface of the glycine crystal, Ra roughness value of the area 1.15 nm. e) Water washed surface of a glycine crystal from the surface of the same crystal as in Fig. 5b (IV), the Ra roughness 9.6 nm. f) Water washed surface of a glycine crystal the Ra roughness was 4.78 nm.

The AFM images from the pure glycine slice surfaces showed a step structure, which was aligned generally in the same direction as the steps in the optical microscope images. The orientation of the steps was mainly along the longer axis of the crystal (IV, Fig. 1a). The step structures seen in the AFM images (~1 nm) were much smaller in scale than the steps seen in the optical microscope or laser profilometer images (tens to hundreds nanometers). The step heights in all of the crystals had thicknesses from single to multiple (1 nanometer to couple of

nanometres) molecule layers. In the AFM images, there were also sharp edges due to the cleaving of the crystals. These results were in agreement with the findings of Carter et al. since the step heights (single step 8.9 Å) and the orientation of the steps seemed to be similar (Carter et al. 1994). The sharp edges were most likely due to cleaving as mentioned above.

The use of crystal structure visualization software such as Mercury, made it easier to understand why α-glycine crystals can be cleaved in along the [010] slip plain. In the α-glycine structure is a bi-layer structure where there is a weaker bonding between the molecules of the bi-layers. In addition, the crystal structure visualization helps to understand what kinds of crystal step heights can be expected of the cleaved surface since it is possible to measure distances within the structures. The AFM imaging is able to image the crystal surface structure in detail this can give information about the growth of the crystal. Quite often, the surfaces of the real crystals have a large number of defects which originate from e.g. cleaving and crystal structure defects. The defects on crystal surfaces can make the interpretation of the surface image difficult.

The effect of ethanol washing treatment on the glycine crystal surface was much larger on the AFM scale than optical microscope or laser profilometer scale (Fig. 8). Ethanol washing dissolved nearly all the small step structures from the surface of the crystal, even though glycine is poorly soluble in ethanol. The new crystallized surfaces were quite heterogeneous and had many different kinds of areas on the surfaces. There were growth hillocks in some areas and some 2D nucleation were visible. The smallest step heights in the hillocks were ~1 nm high which was in good agreement with the thickness of a single bi-layer (8.9 Å). In addition, small 2D islands could be found on the top of the larger steps. These 2D islands were about 1 nm high and microns in diameter. The water washing modified the surfaces

totally in the laser profilometer and in the AFM scale. In some places, the roughness increase with water washing was reasonably close to that seen with ethanol washing, but in other places the surface became unmeasureable since the roughness increased so dramatically or the whole area dissolved away. Water washing changed the surface more than ethanol washing since glycine is very soluble in water and water evaporates much slower than ethanol resulting in a longer contact time.

The AFM can reveal many nanometer scale details from the crystal surfaces that optical imaging methods cannot see. Many surfaces look very homogeneous under optical microscopy, but when the area is imaged with AFM a whole new world is revealed. AFM is a slow technique (one image 5-10 minutes) and covers a very small area (maximum of 100 µm x 100 µm) at the time so a very limited area can be imaged. Due to the area size and roughness limitations AFM measurements are largely dependent on the selection of the place where the measurements are made. The complete surface or even majority of the surface area cannot be covered by the AFM, therefore one has to select places where to measure. This influences the image and roughness information received by the AFM.

6.4. The surface roughness of powder compacts

6.4.1 Standard roughness measurements

In this chapter surface roughness parameters have been calculated in a way they in the standards like ASME (ASME 1995). Laser profilometer roughness values from the first powder compact study (I) suggested that KCl compacts were smoother than NaCl compacts (I, Table 1). The roughness values measured in the second study (II) (with the standard method) showed that the compact surface roughness increased in the order of KCl < NaCl <

theophylline anhydrate < lactose monohydrate (Table 2). As mentioned above the higher compression pressure decreased the roughness of the compacts, this has already been shown with some tablet surfaces using laser profilometer measurements (Podczeck 1998, Riippi et al.1998; Narayan and Hancook 2003). The Ra values of the KCl compacts were smaller than the Ra values of the NaCl compacts made with the same compression pressure (I-II). Similarly, theophylline compacts were also smoother than similar lactose compacts and both organic materials yielded rougher compacts than the ionic crystals (II). The all the Rq values (I and II) were larger than Ra values, which was especially the case in the 30 kN NaCl compacts (see below). The difference tells about the amount of sharp peaks and valleys on the surfaces. If the Rq is larger than Ra, there are high peaks or deep valleys on the surface, which have relatively small surface area compared to the whole measurement area. Variations in Rp-v values (I) were large and the results overlap each other. Therefore, Rp-v values of the laser profilometer did not give good reliable information about the roughness. The difference in all the roughness values between KCl 80 kN and KCl 30 kN compacts was statistically negligible (I), but between others the difference existed.

The reflection problems with the 30 kN NaCl compacts (I-II) surface already mentioned caused some error points in the height data. These error points caused some high values (outliers) in to the data, which can be seen as a larger difference between Ra and Rq values (I) (30 kN NaCl Ra 0.63 µm / Rq 1.67 µm, 80 kN NaCl Ra 0.33 µm / Rq 0.46 µm). Images drawn from the profilometer data helped in finding these reflection points. Similar difference could be seen also in the results of Table 2. The roughness measured by the laser profilometer mainly reflects the roughness caused by the powder particles and their deformation under compression.

Table 2. Ra and Rq roughness values of the compact surfaces (II) made by two compression forces (30 and 80 kN) and calculated using the standard methods (ASME 1995). Measurement area was 2 mm x 2 mm, resolution 1000 points/mm.

Material (kN)	Ra (µm)	Rq (µm)
Lactose monohydrate 30	0.96	1.39
Lactose monohydrate 80	0.56	0.77
Theophylline anhydrate 30	0.7	0.96
Theophylline anhydrate 80	0.42	0.55
KCl 30	0.4	0.6
KCl 80	0.24	0.4
NaCl 30	0.69	1.79
NaCl 80	0.38	0.5

The roughness differences were clear in the line profiles of the lactose monohydrate compacts (II, Fig. 3c-3d). The effect of lower and higher compression pressures on the surface structure in the case of theophylline anhydrate was not as obvious as with lactose monohydrate, but some difference in the roughness of the compacts can be seen in the line profiles (II, Fig. 4c-4f). The particle size of lactose monohydrate was larger and therefore the original particles were more easily detectable on the compact surfaces than with the theophylline anhydrate compacts (II, Fig. 3a-3b and 4a-4b). It should also be pointed out that usually the reflectance images did not give any additional features from the compact surfaces. However, in the case of the theophylline compacts the largest crystals were better visible in the reflectance mode.

6.4.2 New roughness calculation method

In accordance with the Matrix method (II) the roughness values were calculated from the same 2 x 2 mm measurement areas (laser profilometer data) which were divided into 400 small squares. The final roughness calculations were made from the values of the small

squares. The obtained Matrix method roughness values showed that the 30 kN lactose monohydrate compact was the roughest (Table 3). The higher compression pressure made the lactose monohydrate compact clearly smoother, this was also seen in the SEM images (II, Fig. 2a-2d). With theophylline anhydrate compact, the compression pressure had smaller effect on the surface roughness. The variation of roughness in different areas was higher with lactose monohydrate, theophylline anhydrate and with the ionic salts when the lower compression pressure was used. This suggests that there were larger degrees of heterogeneity on the surfaces when compression pressure was lower.

Table 3. Ra and Rq roughness values of the compact surfaces (II) made by two compression forces (30 and 80 kN) and calculated using the matrix method. Measurement area was 2 x 2 mm, which was divided in 400 small squares.

Material (kN)	Ra (µm)	Rq (µm)
	Mean ± SD (n = 400)	Mean ± SD (n = 400)
Lactose 30	0.86 ± 0.31	1.20 ± 0.40
Lactose 80	0.42 ± 0.09	0.58 ± 0.17
Theophylline 30	0.53 ± 0.17	0.70 ± 0.28
Theophylline 80	0.35 ± 0.05	0.45 ± 0.08
KCl 30	0.25 ± 0.12	0.36 ± 0.25
KCl 80	0.14 ± 0.14	0.21 ± 0.23
NaCl 30	0.61 ± 0.84	1.00 ± 1.33
NaCl 80	0.27 ± 0.07	0.36 ± 0.10

The higher compression pressure made the surface more homogeneous by filling the holes between surfaces with smaller fragmented particles. The compacts made of KCl and NaCl showed that they were smoother than the lactose monohydrate compacts, but the difference in surface roughness between NaCl and theophylline anhydrate was small. A comparison of the roughness value data using the standard and the new matrix method roughness values seems to suggest that in one special case our new method will give higher roughness values for the

30 kN NaCl compacts than for the 30 kN theophylline anhydrate compacts. However, the standard deviation is especially high with 30 kN NaCl compacts and therefore such reasoning is not statistically significant. The high standard deviation is presumably due to the reflection problems of the laser beam from the NaCl compacts surface since the largest holes can result in discontinuities in laser-beam reflection. These discontinuities can cause small artefacts in the images. If the laser profilometer looses surface focus (= discontinuity), the sensor moves rapidly up and down trying to re-establish the surface focus. This up and down movement causes typically one high and one low value, which are not necessary true.

The roughness maps drawn from the roughness values of the Matrix method (II) agree with the laser profilometer images and the line profiles (Fig. 9). When the original laser profilometer images show holes or high peaks, the roughness maps show large local roughness. These roughness maps also show surface heterogeneity, the distribution of the roughness and the shade of the colour shows the scale of roughness (dark – small roughness, bright – large roughness). The roughness maps condense the amount of information given by the laser profilometer images, which makes it easier to see the local roughness differences and the scale of roughness in the measurement area. This also helps the comparison of different measurements. Dividing the measured area into small squares removes the effect of large-scale height variations like uneven powder flow or uneven distribution of the powder in the tablet die. This visualisation technique makes it possible to observe roughness features that were caused by particle size and local compression pressure.

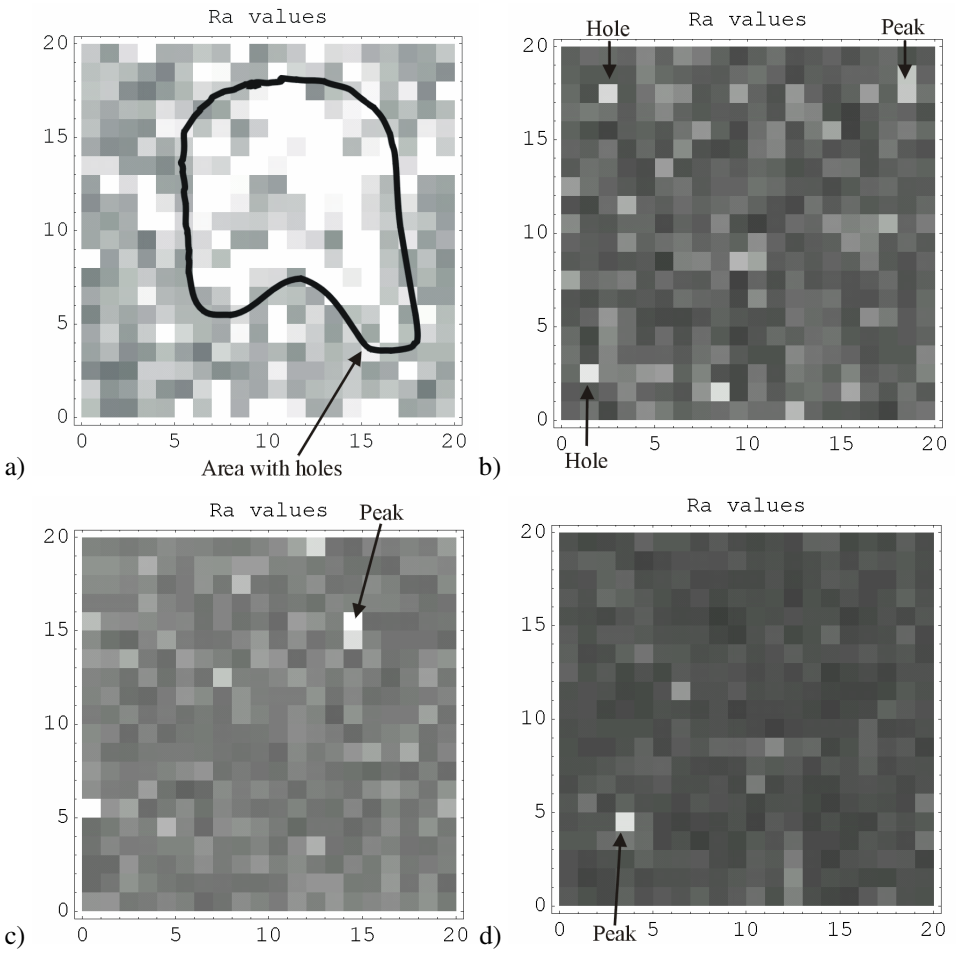

Figure 9. Roughness value maps from the laser profilometer measurements of the powder compacts. The shade of the colour shows the scale of roughness (dark – small roughness, bright – large roughness a) 30 kN lactose monohydrate compact (Ra range 0.48–2.60 µm, mean value 0.86 µm), b) 80 kN lactose monohydrate compact (Ra range 0.27–0.91 µm, mean value 0.42 µm), c) 30 kN theophylline anhydrate compact (Ra range 0.40–3.28 µm, mean value 0.53 µm) and d) 80 kN theophylline anhydrate compact (Ra range 0.26–0.89 µm, mean value 0.35 µm).

With our new Matrix method it is also possible to calculate the roughness values for small squares so that the squares would, more or less, overlap each other. This overlapping of the squares increases the calculation time tremendously and therefore we have not used it in this study. The size of the measurement square that dictates the resolution significantly influences the scale of the roughness values, like in all roughness measurements (Poon and Bhushan

1995; Zahouani et al. 1998). When the size of the square was changed gradually from 2000 x 2000 to 5 x 5 point, the fractal nature of the calculation was revealed (II, Fig. 6) (Yoshinobu et al. 1994; Fang et al. 1997). The drawn lines show the common scaling behaviour, which divides the curve into regions by the size of the square (II, Fig. 6) (Yoshinobu et al. 1994). Furthermore, it is possible to extend the Matrix method easily for other roughness parameters or fractal dimensions and get the visual images of the local variations of these parameters. The method described is not limited to the presented measurement technique or to the scale used in this study. The method described can be used with any roughness measurement which produces numeral data e.g. atomic force microscopy.

The roughness maps cannot be used without an other image showing the true surface topography since the maps does not show is rough area a peak or a valley. The map is description of the roughness calculations not description of the physical surface. If the roughness values in the maps are scaled to a certain scale limit like in this study (between 0 and 1), the maps tell the scale of the roughness in comparison to an other map scaled in the same way. The scaling is not compulsory, but it enhances the colour differences if the roughness differences are small. A care must be taken in the selection of the map square size since it is possible that a valley or a peak is seen as flat area if the map square area matches the surface feature.

6.4.3 AFM roughness measurements

AFM roughness measurements on the compacts (I) were made for a 90 by 90 µm flat areas (n=4) on the compact surfaces. As mentioned above these areas were chosen to be flat areas on the surfaces. The AFM images presented in IV were taken from smaller 10 µm x 10 µm

area in order to get higher resolution (I, Fig. 5). AFM roughness values suggested that KCl compacts were smoother than NaCl compact as in the case of the laser profilometer (I, Table 2). As the other results have suggested above, the higher compression pressure decreases the roughness of the surface. Peak to valley height (Rp-v) values (from lowest point to highest point) measured with AFM gave similar results as the Ra and Rq values. The Rq values were slightly higher than Ra values, which was due to some sharp valleys and peaks on the surface. A similar phenomenon is discussed above in chapter 6.4.1 in the case of laser profilometer roughness data. The results in Rq and Rp-v values between KCl 30 kN and NaCl 80 kN compact overlap, but there was a small difference between the Ra values. Since the AFM measurements were made on the top of the "particles" as explained above, the AFM roughness data reflects only the roughness of single crystalline particles on the surface and their deformation under the compression, not the roughness of the whole compact.

The roughness measurements complement the AFM image information and give quantitative information about height differences. The laser profilometer roughness data reflects the roughness of the whole compact and the AFM roughness data is limited to the roughness of single crystalline particles.

6.5. The surface roughness of the coated tablets

The core tablets (III) were reasonably smooth and the average roughness of the cores was 1.53 ± 0.16 µm. When the coating process began, the surface roughness also started to increase (Fig. 10). Changes in roughness already started to appear after 2.5 minutes of the process time, even though a very small amount of polymer solution was applied. The increase of roughness at the beginning was most likely due to the dissolution effect of the polymer

solution and mechanical wear caused by the mixing in the coater drum (Rowe 1988). The increase in roughness was greatest before the 15 minute point. Between 15 and 30 minutes the roughness increase was smaller, but the variation in the results was large. According to the SEM images and the EDX results, this was the same time period when the coating covered the surface completely. Our findings were quite similar to the earlier studies of Podczeck et al. who also monitored the film coating with a laser profilometer and SEM (Podczeck et al. 1999b). Podczeck et al. found that it took roughly 30 minutes to achieve a fully covering coating. The roughness of the tablets clearly increased this is a quite common known feature (Rowe 1978). The coated tablets from batches without and with pigment did not have any statistical difference in roughness, this was also predicted since the amount of pigment was reasonably small (Rowe 1978).

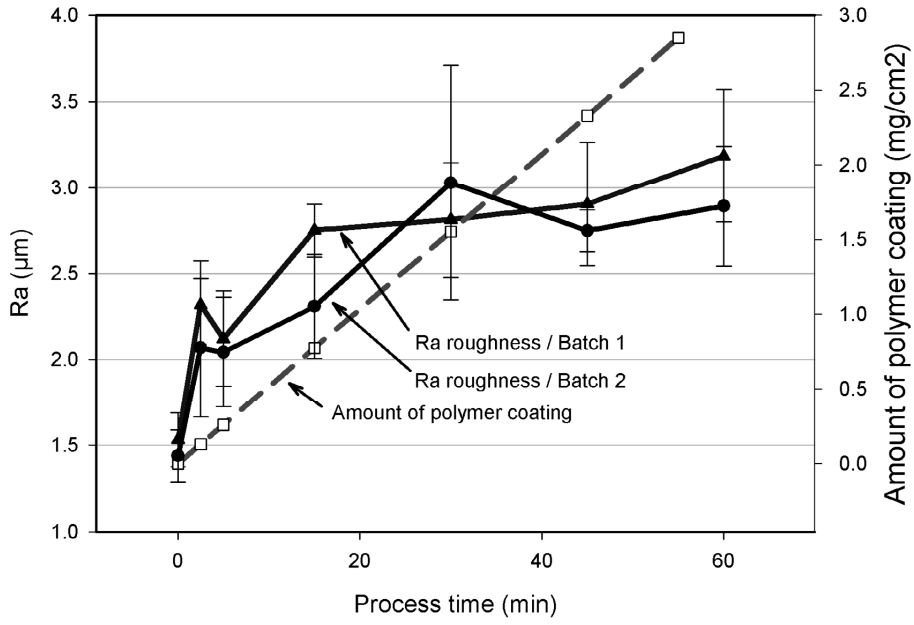

Figure 10. Laser profilometer roughness values and theoretical amount of polymer coating on the tablet surface as a function of process time in a side-vented drum coater. Key: Batch 1 unpigmented film coatings (n = 6) and Batch 2 pigmented film coatings (n = 6). The broken line illustrates the theoretical amount of coating polymer applied (mg/cm^2) as a function of time.

The laser profilometer is a non-invasive technique that gives quantitative 3D information about the tablet surface. With this technique, the measurement is possible when the surface reflects more than 5% of the initial laser light. In the present study, gold sputtering was not needed on the tablet surfaces, since we were confident that laser light reflected back sufficiently from the developing polymer film surface. However, Chopra et al. (2002) used gold sputtering in their study when they measured the surface roughness of polymer coated pellets (Chopra et al. 2002). The reflection information of the profilometer can be used to follow the progress of the surface properties in a qualitative manner. A care must be taken when using the reflection information since the surface roughness also affects the reflection, not only surface material properties like colour.

6.6. The surface roughness of the crystals

The roughness of the pure cleaved crystal surface (IV) varied significantly in the laser profilometer measurements, because of the rather rough cleaving process. The Ra roughness values ranged from 0.03 µm to almost 0.4 µm, this also includes some outliers. The variation was linked directly to the cleaving of the crystal. The most common average roughness (Ra) values (area 0.5 mm x 1.5 mm, resolution 125 points/mm) for the pure glycine surfaces were in the region of 0.1-0.2 µm. The average Ra roughness for a pure glycine surface was 0.15 µm. Because of the large variations, it is necessary to measure the roughness from the same area before and after washing in order to get a better view of the roughness changes. The large roughness differences of the pure glycine surfaces made the statistical comparison difficult, but despite large variations in the laser profilometer measurements, they gave a reasonable good description of the roughness of the whole crystal slice before and after washing.

Ethanol treatment did not have a large effect on the surface roughness when measured with a laser profilometer. In most of the cases, the roughness showed a small (± 10 %) increase, but there were also cases where the roughness decreased slightly. After ethanol washing the Ra roughness values were in the region of 0.1-0.2 µm. The average Ra roughness for ethanol washed glycine surfaces was 0.16 µm. The laser profilometer could not find any statistical roughness difference between the pure glycine surface and the ethanol washed surface. This was most likely linked to the low solubility of glycine to ethanol.

As mentioned above water washing treatment yielded a larger increase in roughness than ethanol. The result of the water washing was greatly dependent on how well the water droplet was spread on the surface. In a couple of tests, the water droplet was not spread on the surface and result was a large cavity on the spot where the droplet was situated. The increase in roughness in water washing varied from about a 20% increase to a 100-time increase, depending on how the droplet was spread on the surface. The water washing affected to the surface in a larger extent and the roughness values were usually between 0.5-1.5 µm, the average value being 0.82 µm.

Optical instruments which have a theoretical maximum resolution of 1 µm, can not see the small scale process on the crystal surface. On the other hand, the optical methods can cover the whole crystal surface at one time to give statistics for the whole crystal. The effect of ethanol washing on surface roughness was small at least on the micrometer scale. The effect of water on the glycine surface was on the other hand so large that it could be seen very clearly with a optical microscope and with laser profilometer. The change in the surface roughness can have significant effects on surface properties such as contact angle (Peltonen et al. 2004). The optical microscope is a very valuable tool in crystal imaging, because it fast

and easily accessible, but it lacks the laser profilometers ability to give 3D numerical data about the surface.

The surface roughness after ethanol washing increased markedly on the AFM scale, but the increase was greatly dependent on the place where the measurement was made. It was difficult to give an accurate description of how much the surface roughness increased. The reason for this was the surface heterogeneity and the small measurement areas in comparison with the size of the whole crystal surfaces. In the optical microscope images before and after washing, many of the crystal surface features were visible (IV, Fig. 3a and 3b). In the AFM images from the same area (as in Fig. 3a and 3b, IV) the surface looked quite different and the roughness had increased greatly after the washing (Fig. 8). Water washing modified the surfaces totally in the laser profilometer and in the AFM scale as mentioned above. The change in surface roughness was at least 10 fold compared to a pure glycine surface.

7. Conclusions

In this study the specific findings were:

1. Optical microscopy is still a very efficient technique, which yields information that SEM and AFM imaging are not able to provide. Roughness measurements complement the image data by giving quantitative information about height differences. AFM roughness data represents the roughness of a single crystalline particle and therefore it needs other methods like laser profilometer to provide broader description of the surface.

2. The new method visualises surface roughness by giving detailed roughness maps. The roughness maps show local variations in surface roughness values and provide a picture of the surface heterogeneity and the scale variation of the roughness between the samples.

3. The laser profilometer results showed that the increase in surface roughness was largest during the first 30 minutes of spraying when the surface was not yet fully covered with coating. The scanning electron microscopy images and the dispersive X-ray analysis results showed that the surface was fully covered with coating within 15 to 30 minutes. The combination of the different measurement techniques made it possible follow the change of surface roughness and development of polymer coating.

4. The optical imaging techniques gave a good overview of the processes affecting the whole crystal surface, but they lacked the resolution to see small nanometer scale processes. AFM was used to visualize the nanoscale effects of cleaving and reveal the full surface heterogeneity which underlies the optical imaging. Ethanol washing changed small (nanoscale) structure to some extent, but the effect of ethanol washing on the larger scale was small. Water washing caused total reformation of the surface structure at all levels

References

Abendan, R.S. and Swift, J.A. 2005.Dissolution on Cholesterol Monohydrate Single-Crystal Surfaces Monitored by in Situ Atomic Force Microscopy. Crys. Growth Des. 5(6), 2146-2153.

Adolfsson, A. and Nyström, C. 1996. Tablet strength, porosity, elasticity and solid state structure of tablets compressed at high loads. Int. J. Pharm. 132(1-2), 95-106.

Aguilera, J.M. and Stanley, D.W. 1999. Microstructural Principles of Food Processing and Engineering (2nd Edition). Aspen Publishers Inc., MA, USA.

Arvidsson, A., Milleding, P., Wennerberg, A. 2002. The influence of a chemo-mechanical caries removal solution on the topography of dental ceramic materials. Biomaterials 23(19), 3977-3983.

ASME 1995, American National Standard, ASME B-46.1-1995.Surface Texture. The American Society of Mechanical Engineers New York, USA.

Barthlott, W. and Neinhuis, C. 1997. Purity of the sacred lotus, or escape from contamination in biological surfaces. Planta, 202, 1-8.

Bashaiwoldu, A.B., Podczeck, F. and Newton, J.M. 2004a. The application of non-contact laser profilometry to the determination of permanent structural changes induced by compaction of pellets: I. Pellets of different composition. Eur. J. Pharm.Sci. 21(2-3), 143-154.

Bashaiwoldu, A.B., Podczeck, F. and Newton, J.M. 2004b. The application of non-contact laser profilometry to the determination of permanent structural change induced by compaction of pellets: II. Pellets dried by different techniques. Eur. J. Pharm.Sci 22(1), 55-61.

Beach, E.R., Tormoen, G.W., Drelich, J. and Han, R. 2002. Pull-off Force Measurements between Rough Surfaces by Atomic Force Microscopy. J. Colloid Interface Sci. 247, 84-99.

Bhushan, B. 2001. Surface Roughness Analysis and Measurement Techniques. In book: Modern tribology handbook Volume I&II. EDS. Bhushan, B. CRC Press Inc., Boca Raton, Florida, USA.

Bindell, J.B. 1992 Scanning Electron Microscopy. In: Encyclopedia of Materials Characterization - Surfaces, Interfaces, Thin Films Edited by: Brundle, C.R., Evans, C.A., Wilson, S. Butterworth-Heinemann, MA, USA.

Binnig, G. and Rohrer, H. 1982. Scanning tunnelling microscope. Helv. Phys. Acta 55, 726-735.

Binnig, G., Quate, C.F. and Gerber, Ch. 1986. Atomic force microscope. Phys. Rev. Lett. 56(6), 930-933.

Bolhuis, G.K. and Chowhan, Z.T. 1996. Materials for direct compaction. In: Pharmaceutical Powder Compaction Technology. Eds. Alderborn, G. and Nyström, C., Marcel Dekker Inc., New York, USA, 461-500.

Bollen, C.M.L., Papaioanno, W., Van Eldere, J., Schepers, E., Quirynen, M. and van Steenberghe, D. 1996. The influence of abutment surface roughness on plaque accumulation and peri-implant mucositis. Clin. Oral. Imp. Res 7(3), 201-211.

Borg, J. and Sangwal, K. 2004. Study of the orientation and frequency of occurence of elementary steps on the (010) cleavage face of potassium acid phthalate single crystals. Surf. Sci. 555, 1-10.

Blunt, L. and Rosén, B.-G. 2001. Topography Instrumentation. In: Metrology and Properties of Engineering Surfaces. Eds. Mainsah, E., Greenwood, J.A., Chetwynd, D.G. Kluwer Academic Publishers Inc., MA, USA.

Brown, A.J.C. 1995. Rapid optical measurement of surfaces. Int. J. Mach. Tools Manufact. 35(2), 135-139.

Bruning, J.H., Herriot, D.R., Gallagher, J.E., Rosenfeld, D.P., White, A.D. and Brangaccio, D.J. 1974. Digital wavefront interferometer for testing optical surfaces and lenses. Appl. Opt. 13(11), 2693-2703.

Butt, H.-J. and Kuropka, R. 1995. Surface structure of latex films, varnishes, and paint films studied with an atomic force microscope. J. Coat. Technol. 67(848), 101-107.

Caber, P. J. 1993. An Interferometric Profiler for Rough Surfaces. Appl. Opt. 32(19), 3438-3441.

Carter, P.W., Hillier, A.C. and Ward, M.D. 1994. Nanoscale Surface Topography and Growth of Molecular Crystals: The Role of Anisotropic Intermolecular Bonding. J. Am. Chem. Soc. 116, 944-953.

Chappard, D., Degasne, I., Hure, G., Legrand, E., Audran, M. and Basle, M.F. 2003. Image analysis measurements of roughness by texture and fractal analysis correlate with contact profilometry. Biomaterials 24(8), 1399-1407.

Chauvy, P.F., Madore, C. and Landolt, D. 1998. Variable length scale analysis of surface topography: characterization of titanium surfaces for biomedical applications. Surf. Coat. Technol. 110(1-2), 48-56.

Chesters, S., Wang, H.C. and Kasper, G. 1991. A fractal-based method for describing surface texture. Solid State Tech. 34(1), 73-77.

Chinga, G. 2002. Structural studies of LWC paper coating layers using SEM and image analysis techniques. Ph D. Thesis February 2002. Norwegian University of Science and Technology Department of Chemical Engineering.

Chopra, R., Podczeck, F., Newton, J.M. and Alderborn, G. 2002. The influence of film coating on the surface roughness and specific surface area of the pellets. Part. Part. Syst. Charact.19, 277-283.

Church, E. L. 1979. The measurement of surface texture and topography by differential light scattering. Wear 57(1), 93-105.

Cochrane, D.J. 2000. Stainless steel finishes – Options and application. Presentation at Symposium Stainless steel in Architectur 15th June 2000, Berlin, Germany. (www.euro-inox.org/pdf/paper/Cochrane_EN.pdf).

Conceição, S., Santos, N.F., Velho, J. and Ferreira, J.M.F. 2005. Properties of paper coated with kaolin: The influence of the rheological modifier. Appl. Clay Sci. 30(3-4), 165-173.

Danesh, A., Connell, S.D., Davies, M.C., Roberts, C.J., Tendler, S.J.B., Williams, P.M. and Wilkins, M.J. 2001. An In Situ Dissolution Study of Aspirin Crystal Planes (100) and (001) by Atomic Force Microscopy. Pharm. Res., 18(3), 299-303.

Davies, T., Kun, X. and Luxmoore, A.R. 1994. Digital measurement of surface profiles by automated optical sectioning. Meas. Sci. Technol. 5(6), 710-715.

De Witte, M.J.C., De Maeyer, E.A.P. and Verbeeck, R.M.H. 2003. Surface roughening of glass ionomer cements by neutral NaF solutions. Biomaterials 24(11), 1995-2000.

Dupuy, M.O. 1967/68. High-presicion optical profilometer for the study of microgeometrical surface defects. Proc. I. Mech. E., Part K, 182, 255-259.

Ebnesajjad, S. and Khaladkar, P.R. 2005. Fluoropolymers Applications in Chemical Processing Industries - The Definitive User's Guide and Databook. William Andrew Publishing inc., NY, USA.

Eiliazadeh, B., Briscoe, B.J., Sheng,Y. and Pitt, K. 2003. Investigating Density Distributions for Tablets of Different Geometry During the Compaction of Pharmaceuticals. Particul.Sci.Technol. 21(4), 303-316.

El Feninat, F., Elouatik, S., Ellis, T.H., Sacher, E. and Stangel, I. 2001. Quantitative assessment of surface roughness as measured by AFM: application to polished human dentin. Appl.Surf.Sci. 183(3-4), 205-215.

El-Sherbiny, S. and Xiao, H. 2005. Surface characteristics of coated paper improved by plastic pigments and synthetic thickeners. Ind. Eng. Chem. Res. 44, 9875-9883.

Fang, S.J., Haplepete, S., Chen, W., Helms, C.R. and Edwards, H. 1997. Analyzing atomic force microscopy images using spectral methods. J. Appl. Phys. 82, 5891-5895.

Flament, M.-P., Leterme, P. and Gayot, A. 2004. The influence of carrier roughness on adhesion, content uniformity and the in vitro deposition of terbutaline sulphate from dry powder inhalers. Int J. Pharm. 275, 201-209.

Farshad, F.F., Pesacreta, T.C., Garber, J.D. and Bikki, S.R. 2001. A comparison of surface roughness of pipes as measured by two profilometers and atomic force microscopy. Scanning, 23(4), 241-248.

Felton, L. and McGinity, J.W. 1999. Adhesion of polymeric films to pharmaceutical solids. Eur. J. Pharm. Biopharm. 47, 3-14.

Felton, L.A. and McGinity, J.W. 1996. Influence of tablet hardness and hydrophobicity on the adhesive properties of an acrylic resin copolymer. Pharm. Dev. Technol. 1, 381–389.

Fujii, H. and Lit, J.W.Y. 1978. Surface roughness measurement using dichromatic speckle pattern: an experimental study. Appl. Optics. 17 (17), 2690-2694.

Garini, Y., Vermolen B.J. and Young, I.T. 2005. From micro to nano: recent advances in high-resolution microscopy. Curr. Opin. Biotechnol. 16(1), 3-12.

Geiss, H. 1992. Energy-dispersive x-ray spectroscopy. In: Encyclopedia of Materials Characterization - Surfaces, Interfaces, Thin Films Edited by: Brundle, C.R., Evans, C.A., Wilson, S. Butterworth-Heinemann, MA, USA.

Hamilton, D. K. and Wilson, T. 1982. Three-dimensional surface measurement using the confocal scanning microscope. Appl. Phys., B 27(4), 211-213.

Harasaki, A., Schmit, J. and Wyant, J.C. 2001. Offset of coherent envelope position due to phase change on reflection. Appl. Opt. 40, 2102-2106.

He , L. and Zhu, J. 1997. The fractal character of processed metal surfaces. Wear 208, 17-24.

Healy, A.M., Corrigan, O.I. and Allan, J.E.M. 1995. The effect of dissolution on the surface texture of model solid-dosage forms as assessed by forms by non-contact laser profilometry. Pharm. Tech. Eur. 9, 14-22.

Heng, P. W., Chan, L.W. and Lim, L.T. 2000. Quantification of the surface morphologies of lactose carriers and their effect on the in vitro deposition of salbutamol sulphate. Chem. Pharm. Bull. 48(3), 393-398.

Holgado, M.A., Fernández-Hervás, M.J., Fernández-Arévalo, M. and Rabasco, A.M. 1995. Use of fractal dimensions in the study of excipients: application to the characterization of modified lactoses. Int J. Pharm. 121, 187-193.

Honary, S. and Orafai, H. 2003. The effect of core surface tension on roughness of film-coated tablets. Iranian J. Pharm. Res. 2(1), 65-66.

Hooke, R.1664. Micrographia. Royal Society of London, UK.

Hunsaker, J.C. and Righmire, B.G. 1947. Engineering applications on fluid mechanics. McGraw-Hill, New York, USA.

Hyvärinen, V., Peiponen, K., Silvennoinen, R., Raatikainen, P., Paronen, P. and Niskanen, T. 2000a. Optical inspection of punches: flat surfaces. Eur. J. Pharm. Biopharm. 49(1), 87-90.

Hyvärinen, V., Silvennoinen, R., Peiponen, K.-E. and Niskanen, T. 2000b. Diffractive optical element based sensor for surface quality inspection of concave punches. Eur. J. Pharm. Biopharm. 49(2), 167-169.

Inoeu, T. 2002. Morphology of polymer blends. EDS. Utraki, L.A. Polymer Blends Handbook, Vol. 1-2, Springer – Verlag.

Iida, K., Hayakawa, Y., Todo, H., Okamoto, H., Danjo, K. and Leuenberger, H. 2004. Effects of surface processing of lactose carrier particles on dry powder inhalation properties of salbutamol sulfate. Chem. Pharm. Bull. 52(8), 938-942.

Jacob, J.S. 1999. Characterisation of drug delivery systems. In: Encyclopedia of Controlled Drug Delivery, Volumes 1-2. Eds. Mathiowitz, E. John Wiley & Sons Inc., MA, USA.

Jalili, N. and Laxminarayana, K. 2004. A review of atomic force microscopy imaging systems: application to molecular metrology and biological sciences. Mechatronics 14(8), 907-945.

Jiang, R.G., Pan, W.S., Wang, C.L. and Liu, H. 2005. Use of recrystallized lactose as carrier for inhalation powder of interferon α2b. Pharmazie 60(8), 632-633.

Jones, R., Pollocka, H.M., Geldartb, D. and Verlinden, A. 2003. Inter-particle forces in cohesive powders studied by AFM: effects of relative humidity, particle size and wall adhesion. Powder Tech. 132, 196– 210.

Jones, R., Pollocka, H.M., Geldartb, D. and Verlinden-Luts, A. 2004. Frictional forces between cohesive powder particles studied by AFM. Ultramicroscopy 100, 59–78.

Kaerger, J.S. and Price, R. 2004. Processing of Spherical Crystalline Particles via a Novel Solution Atomization and Crystallization by Sonication (SAXS) Technique. Pharm. Res. 21(2), 372-381.

Kaye, B.H. 1993. Fractal dimensions in data space; new descriptors for fine particle systems. Part. Part. Syst. Charact. 10(4), 191-200.

Kaye, B.H. 1995. Applied fractal geometry and powder technology. Chaos, Solitons & Fractals 6, 245-253.

Kelly, P.J., Arnell, R.D., Hudson, M.D., Wilson, A.E.J. and Jones, G. 2001. Enhanced mechanical seal performance through CVD diamond films. Vacuum 61, 61-74.

Kent, H.J. 1991. The fractal dimension of paper surface topography. Nordic Pulp Paper Res. J., 6(4), 191-196.

Khan, H., Fell, J.T. and Macleod, G.S. 2001. The influence of additives on the spreading coefficient and adhesion of a film coating formulation to a model tablet surface. Int. J. Pharm. 227, 113–119.

Kiang, Y.-H., Shi, H.G., Mathre, D.J., Xu, W., Zhang, D. and Panmai, S. 2004. Crystal structure and surface properties of an investigational drug—A case study. Int. J. Pharm. 280, 17–26.

Kiely, J.D. and Bonnell, D.A. 1997. Quantification of topographic structure by scanning probe microscopy. J. Vacuum Sci. Tech., B 15(4), 1483-1493.

Kloss, S., Mueller, U. and Oelschlaeger, H. 2005. Studies on the recovery of pharmaceutical drug substances from surfaces made of defined stainless-steel alloys. Pharmazie 60(9), 661-664.

Krim, J., Heyvaert, I., Van Haesendonck, C. and Bruynseraede, Y. 1993. Scanning tunneling microscopy observation of self-affine fractal roughness in ion-bombarded film surfaces. Phys. Rev. Lett. 70(1), 57-60.

Krogars, K., Heinamäki, J., Antikainen, O., Karjalainen, M. and Yliruusi. J. 2002. Tablet film-coating with amylose-rich maize starch. Eur. J. Pharm. Sci. 17, 23–30.

Krogars, K., Antikainen, O., Heinamäki, J., Laitinen, N. and Yliruusi. J. 2003. A novel amylase corn-starch dispersion as an aqueous film coating for tablets. Pharm. Dev. Tech. 8(3), 211-217.

Kuisma, R., Pesonen-Leinonen, E., Redsven, I., Kymäläinen, H.-R. Saarikoski, I. Sjöberg, A.-M. and Hautala, M. 2005. Utilization of profilometry, SEM, AFM and contact angle measurements in describing surfaces of plastic floor coverings and explaining their cleanability. Surf. Sci., 584(1), 119-125.

Koura, M.M. and Omar, M.A. 1981. The effect of surface parameters on friction. Wear 73, 235-246.

Kwok, T.S.H., Sunderland, B.V. and Heng, P.W.S. 2004 An investigation on the influence of a vinyl pyrrolidone/vinyl acetate copolymer on the moisture permeation, mechanical and adhesive properties of aqueous-based hydroxypropyl methylcellulose film coatings. Chem. Pharm. Bull. 52(7), 790-796.

Le, H.R. and Sutcliffe, M.P.F. 2000. Analysis of surface roughness of cold-rolled aluminum foil. Wear 244, 1-2, 71-78.

Li, T., Park, K. 1998. Fractal analysis of pharmaceutical particles by atomic force microscopy. Pharm.Res. 15(8), 1222-1232.

Lin, F. and Meier, D.J. 1995. A study of latex film formation by atomic force microscopy. 1. A comparison of wet and dry conditions. Langmuir 11, 2726-2733.

Liu, J. and Williams R.O. 2002. Properties of heat-humidity cured cellulose acetate phthalate free films. Eur. J. Pharm. Sci. 17, 31–41.

Louey, M.D., Mulvaney, P. and Stewart, P.J. 2001.Characterisation of adhesional properties of lactose carriers using atomic force microscopy. J. Pharm. Biomed. Anal. 25(3-4), 559-567.

Louey, M.D., Razia, S. and Stewart, P.J. 2003. Influence of physico-chemical carrier properties on the in vitro aerosol deposition from interactive mixtures. Int.J.Pharm. 252(1-2), 87-98.

Luo, X.P., Silikas, N., Allaf, M., Wilson, N.H.F. and Watts, D.C. 2001. AFM and SEM study of the effects of etching on IPS-Empress 2 dental ceramic. Surf. Sci. 491, 388-394.

Lysenko, S.I., Snopok, B.A., Sterligov, V.A. and Shirshov, Y.M. 2001. Statistical properties of surfaces: features of the calculation of the autocovariance function from the scattering indicatrix. Opt. Spectrosc. 91(5), 801-809.

MacDonald, W., Campbell, P., Fisher, J. and Wennerberg, A. 2004. Variation in surface texture measurements. J. Biomed. Mater. Res., B, 70B(2), 262-269.

Mainsah, E., Stout, K.J. and Thomas, T.R. 2001. Surface measurement and characterisation. In: Metrology and Properties of Engineering Surfaces. Eds. Mainsah, E., Greenwood, J.A., Chetwynd, D.G. Kluwer Academic Publishers Inc., MA, USA.

Majumdar, A. and Bhushan, B. 1999. Characterization and modelling of surface roughness and contact mechanics. In: Handbook of Micro/Nanotribology. Ed. Bhushan, B. CRC Press LLC, Boca Raton, USA.

Mandelbrot, B.B. 1983. The fractal geometry of nature, 3rd Edition, Freeman, NY, USA.

Marsh, R.E. 1958. A refinement of the crystal structure of glycine. Acta Crystallogr 11, 654-663.

Merrett, K., Cornelius, R.M., Mcclung, W.G., Unsworth, L.D. and Sheardown. H. 2002. Surface analysis methods for characterizing polymeric biomaterials. J. Biomater. Sci. Polymer Edn., 13(6), 593-621.

Ming, W., Wu, D., van Benthem, R. and de With, G. 2005. Superhydrophobic Films from Raspberry-like Particles. Nano Lett. 5 (11), 2298 -2301.

Missaghi, S. and Fassihi, R. 2004. A novel approach in the assessment of polymeric film formation and film adhesion on different pharmaceutical solid substrates. AAPS PharmSciTech. 5(2), article 29 (http://www.aapspharscitech.org).

Mizes, H. A.. 1995. Surface roughness and particle adhesion. J. Adhesion 51(1-4), 155-165.

zur Muhlen,A., zur Muhlen,E., Niehus,H. and Mehnert,W. 1996. Atomic force microscopy studies of solid lipid nanoparticles. Pharm. Res. 13, 1411-1416.

Muster, T.H.and Prestidge, C.A. 2002. Face specific surface properties of pharmaceutical crystals. J. Pharm. Sci. 91(6), 1432-1444.

Nadkarni, P.D., Kildsig, D.O., Kramer, P.A. and Banker, G.S. 1975. Effects of surface roughness and coating solvent on film adhesion to tablets, J. Pharm. Sci. 64, 1554–1557.

Narayan, P. and Hancock, B.C. 2003. The relationship between the particle properties, mechanical behavior, and surface roughness of some pharmaceutical excipient compacts. Mater. Sci. Eng., A355(1-2), 24-36.

Narayan, P. and Hancock, B.C. 2005. The influence of particle size on the surface roughness of pharmaceutical excipient compacts. Mater. Sci. Eng. A 407, 226–233.

Newton, M., Petersson, J., Podczeck, F., Clarke,A. and Booth, S. 2001. The influence of formulation variables on the properties of pellets containing a self-emulsifying mixture. J. Pharm. Sci. 90(8), 987-995.

Nogueira, I., Dias, A.M., Gras, R. and Progri, R. 2002. An experimental model for mixed friction during running-in. Wear 253, 541–549.

Ohmori, S, Ohno, Y, Makino, T and Kashihara, T. 2004. Improvement of impact toughness of sugar-coated tablets manufactured by dusting method. Chem. Pharm. Bull. 52, 322-328.

Oliva, A.I., Anguiano, E. and Aguilar, M. 1999. Fractal dimension: measure of coating quality. Surf. Eng. 15(2), 101-104.

Oliveira, S.A., Pugach, M.K., Hilton, J.F., Watanabe, L.G., Marshall, S.J. and Marshall, G.W.,Jr. 2003. The influence of the dentin smear layer on adhesion: a self-etching primer vs. a total-etch system. Dent. Mater. 19(8), 758-767.

Palasantzas, G. and De Hosson, J.Th.M. 2003. Influence of surface roughness on the adhesion of elastic films. Phys. Rev. E, 67, 021604.

Pawlus, P. 1997. Change of cylinder surface topography in the initial stage of engine life. Wear 209, 69-83.

Peltonen, J., Järn, M., Areva, S., Linden, M. and Rosenholm, J.B. 2004. Topographical Parameters for Specifying a Three-Dimensional Surface. Langmuir 20(22), 9428-9431.

Peltonen, L., Mannermaa, J.P. and Yliruusi, J. 1997. Roughness analysis from tablet surfaces with a confocal laser scanning microscope. Pharmazie 52(11), 860-863.

Pérez, E. and Lang, J. 1999. Flattening of latex film surface: theory and experiments by atomic force microscopy. Macromol. 32, 1626-1636.

Persson, B. N. J., Albohr, O., Tartaglino, U., Volokitin, A .I. and Tosatti, E. 2005. On the nature of surface roughness with application to contact mechanics, sealing, rubber friction and adhesion. J. Phys.: Condens. Matter 17, R1–R62.

Petitgrand, S. and Bosseboeuf, A. 2004 Simultaneous mapping of out-of-plane and in-plane vibrations of MEMS with (sub)nanometer resolution. J. Micromech. Microeng. 14, S97-S101.

Podczeck, F. 1997a. Factors influencing Adhesion. In book: Particle-Particle adhesion in pharmaceutical powder handling. Imperial College Press, London, UK.

Podczeck, F. 1997b. The relationship between particulate properties of carrier materials and the adhesion force of drug particles in interactive powder mixtures. J.Adhes.Sci.Technol. 11(8), 1089-1104.

Podczeck, F. 1998. Measurement of surface roughness of tablets made from polyethylene glycol powders of various molecular weights. Pharm. Pharmacol. Commun. 4, 179-182.

Podczeck, F., Brown, S. and Newton, J.M. 1999a. The influence of powder properties and tabletting conditions on the surface roughness of tablets. Part Part. Syst. Charact. 16, 185-190.

Podczeck, F., Brown, S. and Newton, M. 1999b. Monitoring film coating with surface profilometry. Pharm. Technol. 23, 48-56.

Poon, C.Y. and Bhushan, B. 1995. Comparison of surface roughness measurements by stylus profiler, AFM and non-contact optical profiler. Wear 190(1), 76-88.

Price, R., Young, P.M., Edge, S. and Staniforth, J.N. 2002. The influence of relative humidity on particulate interactions carrier-based dry powder inhaler formulations. Int. J. Pharm. 246, 47-59.

Qu, J., Truhan, J.J., Blau, P.J. and Meyer, H.M. 2005. Scuffing transition diagrams for heavy duty diesel fuel injector materials in ultra low-sulfur fuel-lubricated environment. Wear 259, 1031–1040.

Rasigni, G., Varnier, F., Rasigni, M., Palmari, J. P. and Llebaria, A. 1983. Autocovariance functions for polished optical surfaces. J. Opt. Soc. Am. 73(2), 222-233.

Reiland, T.L. and Eber, A.C. 1986. Aqueous gloss solutions: Formula and process variables effects on the surface texture of film coated tablets. Drug Dev. Ind. Pharm. 12(3), 231-245.

Riippi, M., Antikainen, O., Niskanen, T. and Yliruusi, J. 1998. The effect of compression force on surface structure, crushing strength, friability and disintegration time of erythromycin acistrate tablets. Eur. J. Pharm. Biopharm. 46, 339-345.

Rissa, K. and Lepistö, T. 2000. Orientation of talc particles in dispersion coatings. Nordic Pulp Paper Res. J. 15, 357-361.

Roberts, M., Ford, J.L., MacLeod, G.S., Fell, J.T., Smith, G.W. and Rowe, P.H. 2003. Effects of surface roughness and chrome plating of punch tips on the sticking tendencies of model ibuprofen formulations. J. Pharm. Pharmacol. 55(9), 1223-1228.

Roberts, R.J. and Rowe, R.C. 1986. The effect of the relationship between punch velocity and particle size on the compaction behaviour of materials with varying deformation mechanisms, J. Pharm. Pharmacol. 38, 567-571.

Rohera, B.D and Parikh, N.H. 2002. Influence of plasticizer type and coat level on surelease film properties. Pharm. Dev. Tech. 7, 407-420.

Rowe, R.C. 1977. The adhesion of film coatings to tablet surfaces: the effect of some direct compression excipients and lubricants. J. Pharm. Pharmacol., 29(12), 723-726.

Rowe, R.C. 1978. The measurement of the adhesion of film coatings to tablet surfaces: the effect of tablet porosity, surface roughness, and film thickness. J. Pharm. Pharmacol. 30(6), 343–346.

Rowe, R. C. 1979. Surface roughness measurements on both uncoated and film-coated tablets. J. Pharm. Pharmacol. 31(7), 473-474.

Rowe, R.C. 1985a. Appearance measurements on tablets. Pharm. Int. 6(9), 225-230.

Rowe, R.C. 1985b. Gloss measurement on film coated tablets. J Pharm. Pharmacol. 37(11), 761-765.

Rowe, R.C. 1988. Tablet-tablet contact and mutual rubbing within a coating drum – an important factor governing the properties and appearance of tablet film coatings. Int. J. Pharm. 43, 155-159.

Ruotsalainen, M., Heinämäki, J, Antikainen, O. and Yliruusi, J. 2002a. Time-dependent dimensional changes and film adhesion of coated tablets. S.T.P. Pharm. Sci. 12(6), 385-389.

Ruotsalainen, M., Heinämäki, J., Rantanen, J. and Yliruusi, J. 2002b. Development of an automation system for a tablet coater. AAPS PharmSciTech 3(2), article 14 (http://www.aapspharscitech.org).

Ruotsalainen, M., Heinamaki, J., Guo, H., Laitinen, N. and Yliruusi, J. 2003a. A novel technique for imaging film coating defects in the film-core interface and surface of coated tablets. Eur. J. Pharm. Biopharm. 56(3), 381-388.

Ruotsalainen, M., Heinämäki, J, Taipale, K. and Yliruusi, J. 2003b. Influence of the aqueous film coating process on the properties and stability of tablets containing a moisture-labile drug. Pharm. Dev. Tech. 8(4), 443–451.

Russ, J.C. 1994. Fractal surfaces, Plenum Press Corporation, NY, USA.

Russ, J.C. 2001. Fractal geometry in engineering. In: Metrology and Properties of Engineering Surfaces. Eds. Mainsah, E., Greenwood, J.A., Chetwynd, D.G. Kluwer Academic Publishers Inc., MA, USA.

Rönnow, D., Bergkvist, M., Roos, A. and Ribbing, C.-G. 1993. Determination of interface roughness by using a spectroscopic total-integrated-scatter instrument. Appl. Optics. 32(19), 3448-3451.

Sandoz, P., Tribillon, G., Gharbi, T. and Devillers, R. 1996. Roughness measurement by confocal microscopy for brightness characterization and surface waviness visibility evaluation. Wear 201, 186-192.

Salako, M., Podczeck, F. and Newton, M. 1998. Investigations into deformability of and tensile strength of pellets. Int. J. Pharm. 168, 19-57.

Sangwal, K., Sanz, F. and Gorostiza, P. 1997. Study of the surface morphology of the (100) cleavage planes of MgO single crystals by atomic force microscopy. Surf. Sci. 383, 78-87.

Shindo, H., Seo, A., Watabe, T. 2001. Structures of the CaSO4(001) surface studied with atomic force microscopy in air and in solution. Phys. Chem. Chem. Phys. 3, 230-234.

Silva, M.H.P., Soares, G.A. and Elias, C.N. 2000. Surface analysis of titanium dental implants with different topographies. Material Research 3(3), 61-67.

Silvennoinen, R., Peiponen, K.-E., Hyvärinen, V., Raatikainen, P. and Paronen, P. 1999. Optical surface roughness study of starch acetate compacts. Int. J. Pharm. 182, 213–220.

Sindel, U. and Zimmermann, I. 2001. Measurement of interaction forces between individual powder particles using an atomic force microscope. Powder Tech. 117, 247-254.

Smith, K.B. 1999. Measuring the perception of glossy surfaces. Pigm. Resin Technol. 28 (4), 217-222.

Song, J.F. and Vorburger, T. V. 1992. Surface Texture. ASM Handbook vol. 18: Friction, Lubrication and Wear Technology, ASM International, Materials Park, OH.

Suihko, E., Lehto, V.-P., Ketolainen, J., Laine, E. and Paronen, P. 2001. Dynamic solid-state and tableting properties of four theophylline forms. Int. J. Pharm. 217, 225-236.

Suzuki, K., Aoki, K. and Ohya, K. 1997. Effects of surface roughness of titanium implants on bone remodeling activity of femur in rabbits. Bone 21(6), 507-514.

Swain, M.V., Lawn, B.R. and Burns, S. J. 1974. Cleavage step deformation in brittle solids. J. Mater. Sci. 9(2), 175-183.

Tandon P.N. and Rakesh, L. 1981. Effects of cartilage roughness on the lubrication of human joints. Wear 70, 29-36.

The Lotus Effect. 2006. Information involving surface roughness in biological systems relation to hydrophobicity and surface self-cleaning in biological systems. Internet site, accessed 16th of January 2006. http://www.botanik.uni-bonn.de/system/bionik flash.html. The Department of Botany, University of Bonn, Germany.

Thomas, T.R. 1999. Rough surfaces 2nd edition, London Imperial College Press, UK

Tiarks, F., Frechen, T., Kirsch, S., Leuninger, J., Melan, M., Pfau, A., Richter, F., Schuler, B. and Zhao, C.-L. 2003. Formulation effects on the distribution of pigment particles in paints. Prog. Org. Coat. 48(2-4), 140-152.

Toyoshima, K., Yasumura, M., Ohnishi, N. and Ueda, Y. 1988. Quantitative evaluation of tablet sticking by surface roughness measurement. Int.J.Pharm. 46(3), 211-215

Trojak, A., Kocevar, K., Musevic, I. and Srcic, S. 2001. Investigation of the felodipine glassy state by atomic force microscopy. Int. J. Pharm. 218(1-2), 145-151.

Twitchell, A.M., Hogan, J.E. and Aulton, M.E. 1995a. Assessment of the thickness variation and surface roughness of aqueous film coated tablets using a light-section microscope. Drug Dev.Ind.Pharm. 21(14), 1611-1619.

Twitchell, A.M., Hogan, J.E. and Aulton, M.E. 1995b. The behaviour of film coating droplets on the impingement onto uncoated and coated tablet. S.T.P. Pharm. Sci. 5, 190-195.

Verran, J., Rowe, D. L. and Boyd, D.R. 2003. Visualization and measurement of nanometer dimension surface features using dental impression materials and atomic force microscopy. Int. Biodeterior. Biodegrad. 51(3), 221-228.

Vorburger, T.V. 1992. Methods of Characterizing Surface Topography. In: Tutorials in Optics. Eds. Moore, D.T. Optical Society of America, Washington, DC, USA.

Vorburger, T. V. and Ludema, K. C. 1979. Ellipsometry of rough surfaces. Appl. Optics. 19(4), 561-573.

Vorburger, T.V. and Raja, J. 1990. Surface Finish Metrology Tutorial, NISTIR 89–4088. National Institute of Standards and Technology, Gaithersburg, MD, June 1990.

Vorburger, T.V. and Teague, E.C. 1981. Optical techniques for on-line measurement of surface topography. Precis. Eng. 3(2), 61-83.

Wagberg, P. and Johansson, P.Å. 1993. Surface profilometry -- a comparison between optical and mechanical sensing on printing papers. Tappi J. 76 (12), 115-121.

Wang, H., Djurisic, A.B., Chan, W.K. and Xie, M.H. 2005. Factors affecting phase and height contrast of diblock copolymer PS–b-PEO thin films in dynamic force mode atomic force microscopy. Appl. Surf. Sci. 252 (4), 1092–1100.

Ward, S., Perkins, M., Zhang, J., Roberts, C. J., Madden, C.E., Luk, S.Y., Patel, N. and Ebbens, S.J. 2005. Identifying and Mapping Surface Amorphous Domains. Pharm. Res. 22(7), 1195-1202.

Wefers, L. and Schollmeyer, E. 1993. Surface characterization of laser-treated poly(ethylene terephthalate) by optical profilometry and scanning tunneling microscopy. J. Polymer Sci., Part B 31(1), 23-27.

Wen, H., Li, T., Morris, K.R. and Park, K 2004. Dissolution study on aspirin and α-glycine crystals. J. Phys. Chem. B 108, 11219-11227.

Wennerberg, A.1996. On the surface roughness and implant incorporation. PhD thesis, Göteborg University, Sweden.

Wickramasinghe, H.K. 1989. Scanned probe microscopes. Scientific American 260(10), 98-105.

Wyant, J.C. 2002. White Light Interferometry. Proc. SPIE 4737, 98-107.

Wyant, J.C., Koliopoulos, C.L., Bhushan, B. and Basila, D. 1986. Development of a three-dimensional noncontact digital optical profiler. Trans. ASME : J. Trib. 108 (1- 8).

Yoshinobu, T., Iwamoto, A. and Iwasaki, H. 1994. Mesoscopic Roughness Characterization of Grown Surfaces by Atomic Force Microscopy. Jpn. J. Appl. Phys., 33 (Part 2), L67-L69.

Young, P.M., Price, R., Tobyn, M.J., Buttrum, M. and Dey, F. 2003. Investigation into the effect of humidity on drug-drug interactions using the atomic force microscope. J.Pharm.Sci. 92(4), 815-822.

Young, P.M., Price, R., Tobyn, M.J., Buttrum, M. and Dey, F. 2004 The influence of relative humidity on the cohesion properties of micronized drugs used in inhalation therapy. J. Pharm. Sci. 93(3), 753-761.

Zahouani, H., Vargiolu, R., Kapsa, P.H., Loubet, J.L. and Mathia, T.G. 1998. Effect of lateral resolution on topographical images and three-dimensional functional parameters. Wear 219(1), 114-123

Zhang, Y. and Sundararajan, S. 2005. The effect of autocorrelation length on the real area of contact and friction behavior of rough surfaces. J Appl. Phys. 97(10), 103526/1-103526/7.

Zhong, Q., Inniss, D., Kjoller, K. and Elings, V.B.. 1993. Fractured polymer / silica fiber surface studied by tapping mode atomic force microscopy, Surf. Sci. 290, L688-L692.